



12-1982

The Geology and Origin of the Sawyer Uranium Prospect, Live Oak County, Texas

Charles L. Brewster
University of Tennessee - Knoxville

Follow this and additional works at: https://trace.tennessee.edu/utk_gradthes



Part of the [Geology Commons](#)

Recommended Citation

Brewster, Charles L., "The Geology and Origin of the Sawyer Uranium Prospect, Live Oak County, Texas. " Master's Thesis, University of Tennessee, 1982.
https://trace.tennessee.edu/utk_gradthes/576

This Thesis is brought to you for free and open access by the Graduate School at TRACE: Tennessee Research and Creative Exchange. It has been accepted for inclusion in Masters Theses by an authorized administrator of TRACE: Tennessee Research and Creative Exchange. For more information, please contact trace@utk.edu.

To the Graduate Council:

I am submitting herewith a thesis written by Charles L. Brewster entitled "The Geology and Origin of the Sawyer Uranium Prospect, Live Oak County, Texas." I have examined the final electronic copy of this thesis for form and content and recommend that it be accepted in partial fulfillment of the requirements for the degree of Master of Science, with a major in Geology.

Kula C. Misra, Major Professor

We have read this thesis and recommend its acceptance:

ARRAY(0x7f7029c13b80)

Accepted for the Council:

Carolyn R. Hodges

Vice Provost and Dean of the Graduate School

(Original signatures are on file with official student records.)

To the Graduate Council:

I am submitting herewith a thesis written by Charles L. Brewster entitled "The Geology and Origin of the Sawyer Uranium Prospect, Live Oak County, Texas." I have examined the final copy of this thesis for form and content and recommend that it be accepted in partial fulfillment of the requirements for the degree of Master of Science, with a major in Geology.

Kula C. Misra
Kula C. Misra, Major Professor

We have read this thesis and recommend its acceptance:

Kenneth P. Wilber
W. C. Kopp

Accepted for the Council:

Levan Bell
Vice Chancellor
Graduate Studies and Research

THE GEOLOGY AND ORIGIN OF THE SAWYER URANIUM PROSPECT,
LIVE OAK COUNTY, TEXAS

A Thesis

Presented for the

Master of Science

Degree

The University of Tennessee, Knoxville

Charles L. Brewster

December 1982

3065077

ACKNOWLEDGMENTS

I would like to express my sincere appreciation to the Sunoco Energy Development Company for generously providing the drill hole core samples, maps and financial assistance to make this research possible. Special thanks go to Harry Hixon, Jerry Eshbaugh and Ian Northern who were instrumental in arranging Sunoco's support. The study also was supported through research grants from the Sigma Xi Scientific Society and from The University of Tennessee Geology Discretionary Funds.

Several people from various institutions also provided valuable assistance in analytical procedures and in the interpretation of the data. Dr. Clayton Gist of Oak Ridge Associated Universities provided X-ray fluorescence facilities and procedural instruction. Dr. Edward Ripley of Indiana University was highly cooperative in providing sulfur isotope analyses on short notice. The University of Tennessee Department of Metallurgic Engineering provided SEM time and operation assistance free of charge. The interpretation of the analytical results was greatly enhanced by discussions with: Dr. William Galloway, Bureau of Economic Geology, University of Texas at Austin; Dr. Martin Goldhaber, United States Geological Survey; and Fred Busche, Shell Oil Company. I am indebted to all of these people for their assistance.

Finally, I wish to express appreciation to my advisor, Dr. Kula C. Misra, and to my committee members Dr. Otto C. Kopp and Dr. Kenneth R. Walker for their guidance in this thesis project. Also, valuable

advice was provided by Mr. Kem Fronabarger in processing the statistical data. In addition, the thesis manuscript benefited greatly from the patient editorial comments of Renee Brewster.

ABSTRACT

The Sawyer uranium prospect is a subsurface uranium occurrence hosted within the basal Oligocene Catahoula Formation of the Texas coastal plain. The host rocks consist of tuff-ball conglomerate, tuffaceous sandstone and tuffaceous claystone whose geometry and lithological characteristics indicate that they are the products of a crevasse-splay depositional environment. Compositionally, these lithologies are feldspar-depleted litharenites, with the feldspar depletion due to the corrosive, ore-forming processes. These sediments display pedogenic to early diagenetic features including diffuse to discrete micrite nodules, clay cutans, fresh to partially argillized glass shards, clay booklets, authigenic zeolites and sulfides, paleo-soil horizons and calcite cement.

Uranium mineralization occurs throughout the crevasse-splay channel sediments, with the richest accumulations (0.1% to 0.94% U_3O_8) concentrated in the tuff-ball conglomerates at the base of the channel sequences. Uranium is correlatable with anomalous concentrations of Pb, As, Rb and Y within the orebodies. Organic carbon content (0.01% to 0.28%) is uniformly low throughout the ore zone and does not display a significant correlation with uranium mineralization. No uranium minerals were detected by X-ray diffraction techniques; however, SEM energy dispersion analysis shows that uranium occurs as scaly encrustations adsorbed onto the surfaces of favorable mineral grains. The uranium-mineralized lithologies also host an appreciable

amount of iron-disulfide minerals which provide data useful in the interpretation of ore paragenesis.

Textural relationships between framboidal pyrite and ore-stage marcasite overgrowths provide evidence that the host rocks were reduced prior to uranium mineralization. The presence of organic carbon and botryoidal clusters of pyrite framboids suggests that the pre-ore reduction was accomplished by sulfate-reducing bacteria. This pre-ore reduction also resulted in the alteration of detrital ilmenite to pyrite and anatase. Following the initial reduction, the host rocks were invaded by oxygenated, uranium-enriched ground waters creating an oxidation-reduction interface along which uranium and associated trace elements were precipitated. The oxidation of pre-ore pyrite in the alteration tongue released Fe^{2+} and unstable sulfur oxyanions which were then available for further reaction upon entering the redox interface. The Fe^{2+} and free sulfur recombined under acidic conditions to form ore-stage marcasite as fine to coarse aggregates and as overgrowths surrounding framboidal pyrite. $\delta^{34}\text{S}$ values of bulk sulfide samples (-9.9 to +8.4 per mil) support the interpretation of biogenic sulfide precipitation. However, the origin of the reductant responsible for post-ore re-reduction of the alteration tongue is uncertain.

TABLE OF CONTENTS

CHAPTER	PAGE
I. INTRODUCTION	1
II. SAMPLING AND ANALYTICAL TECHNIQUES	5
Core Samples	5
Analytical Techniques	8
Host rock petrology	8
Opaque petrology	8
Scanning electron microscopy	8
X-ray fluorescence analysis	9
Uranium and organic carbon	9
Sulfur isotope analysis	9
X-ray diffraction	10
Electron microprobe energy dispersion analysis	10
III. GEOLOGIC SETTING	11
Regional Geology	11
Catahoula depositional systems	11
Structural development	11
Local Geologic Setting	12
Stratigraphy	12
Crevasse-splay lithofacies	15
Structure	15
IV. HOST ROCKS	16
Petrology	16
Tuff-ball conglomerate	16
Sandstone	16
Claystone	20
Classification	20
Interpretation	22
Diagenesis	23
Diagenetic features	23
Timing of diagenesis	23
V. URANIUM MINERALIZATION	25
Uranium Distribution	25
Associated Trace Elements	25
Organic Carbon	30
Ore Mineralogy	30
Uranium mineralogy	30

CHAPTER	PAGE
Opaque mineralogy	39
Opaque Textures	39
Framboidal pyrite	39
Euhedral pyrite	44
Marcasite overgrowths and aggregates	44
Hematite rims	44
Replacement	45
Sulfur Isotope Analysis	45
VI. DISCUSSION	47
Source of Uranium	47
Uranium release from volcanic ash	47
Release mechanisms	48
Uranium release in the Sawyer area	48
Uranium depletion in Sawyer paleosoils	49
Uranium migration	49
Uranium-Sulfide Paragenesis	50
Pre-ore reduction of the host rocks	50
Framboidal pyrite	50
Sulfidization of ilmenite	51
Ore-stage mineralization	52
Roll-front development	52
Destruction of pyrite	52
Role of unstable sulfur compounds	53
Formation of marcasite	54
Post-ore re-reduction	55
Sulfidization of the altered tongue	55
Possible mechanisms for re-reduction	55
Sulfur isotope interpretation	56
Previous studies	56
Sawyer prospect	57
Paragenesis	59
VII. CONCLUSIONS	62
LIST OF REFERENCES	64
VITA	68

LIST OF FIGURES

FIGURE	PAGE
1. Location of the Sawyer Study Area in South Texas	2
2. Sketch Map of the Sawyer Orebodies Showing the Location of Drill Holes Used in This Study	6
3. Distribution of Core Intervals Sampled for Thin Sections (A), Polished Thin Sections (B), X-Ray Fluorescence Analysis (C), Sulfur Isotope Analysis (D), Scanning Electron Microscopy (E), X-Ray Diffraction Analysis (F), and Electron Microprobe Energy Dispersion Analysis (G)	7
4. Geologic Map of the Sawyer Area in Northeastern Live Oak County Showing Facies Distribution in the Catahoula Formation	13
5. Lithologic and SP Log Correlations Across the Sawyer Core Holes Used in This Study	14
6. Photomicrographs of Thin-Sections in Transmitted Light	17
7. QFR Compositions of Sawyer Lithologies According to Folk's (1974) Classification Scheme	21
8. The Distribution of Catahoula Uranium Mineralization Fronts in Northeastern Live Oak County	26
9. The Distribution of Uranium Mineralization Across the Sawyer Cores Expressed as Chemical Percentage	27
10. Plot of U_3O_8 vs. As Concentrations in 20 Sawyer Core Samples	31
11. Plot of U_3O_8 vs. Rb Concentrations in 20 Sawyer Core Samples	32
12. Plot of U_3O_8 vs. Pb Concentrations in 20 Sawyer Core Samples	33
13. Plot of U_3O_8 vs. Y Concentrations in 20 Sawyer Core Samples	34
14. Plot of U_3O_8 vs. Organic Carbon Content in 28 Sawyer Core Samples	35

FIGURE	PAGE
15. SEM Photomicrographs of Uranium-Enriched Encrustations . .	36
16. Energy Dispersion Spectra Obtained from the Encrustation Illustrated in Figure 15B	38
17. Photomicrographs of Framboidal Pyrite and Sulfidized Ilmenite	40
18. Photomicrographs of Opaque Petrology	42
19. $\delta^{34}\text{S}$ Values for Intervals Used in the Sulfur Isotope Study of the Sawyer Cores	46
20. The Paragenesis of Sawyer Mineralization as Interpreted from Relationships Observed in the Sawyer Core Samples . .	61

LIST OF TABLES

TABLE	PAGE
1. Modal Compositions of the Sawyer Lithologies Given in Percent	19
2. Uranium and Associated Trace Element Concentrations	28
3. Pearson Correlation Coefficients for the Sawyer Trace Element Data Presented in Table 2	29
4. Sulfur Isotope Signatures of Various Geochemical Environments	58

CHAPTER I

INTRODUCTION

The Sawyer uranium prospect represents a roll-front type uranium mineralization hosted within the Oligocene Catahoula Formation in northeastern Live Oak County, Texas (Figure 1). The Catahoula Formation in the Sawyer area consists of fluvial channel-fill and crevasse-splay sediments which host several small uranium orebodies (Galloway, 1977). These orebodies include Mobil's Nell deposit and Conoco's House-Seale, Spoon, Ryan and Dobie deposits. The House-Seale deposit has been described by Galloway and Kaiser (1980) in terms of the petrology, diagenesis, mineralogy, paragenesis, uranium and trace-element distribution. They proposed that the reductant responsible for the precipitation of uranium at the House-Seale deposit was H_2S gas released from the Oakville Fault Zone. This implies a long-distance lateral transmission of H_2S gas because the source of the gas is hydrocarbon accumulations buried at a depth of 11,000 to 16,000 feet (4,000 to 5,000 m), ten miles (16.1 km) downdip from the House-Seale deposit. If the House-Seale deposit is representative of the Catahoula orebodies in northeastern Live Oak County, then all of the deposits should display characteristics consistent with Galloway and Kaiser's inorganic reduction hypothesis.

A genetic relationship between some south Texas uranium deposits and fault associated hydrocarbon accumulations has been suggested by

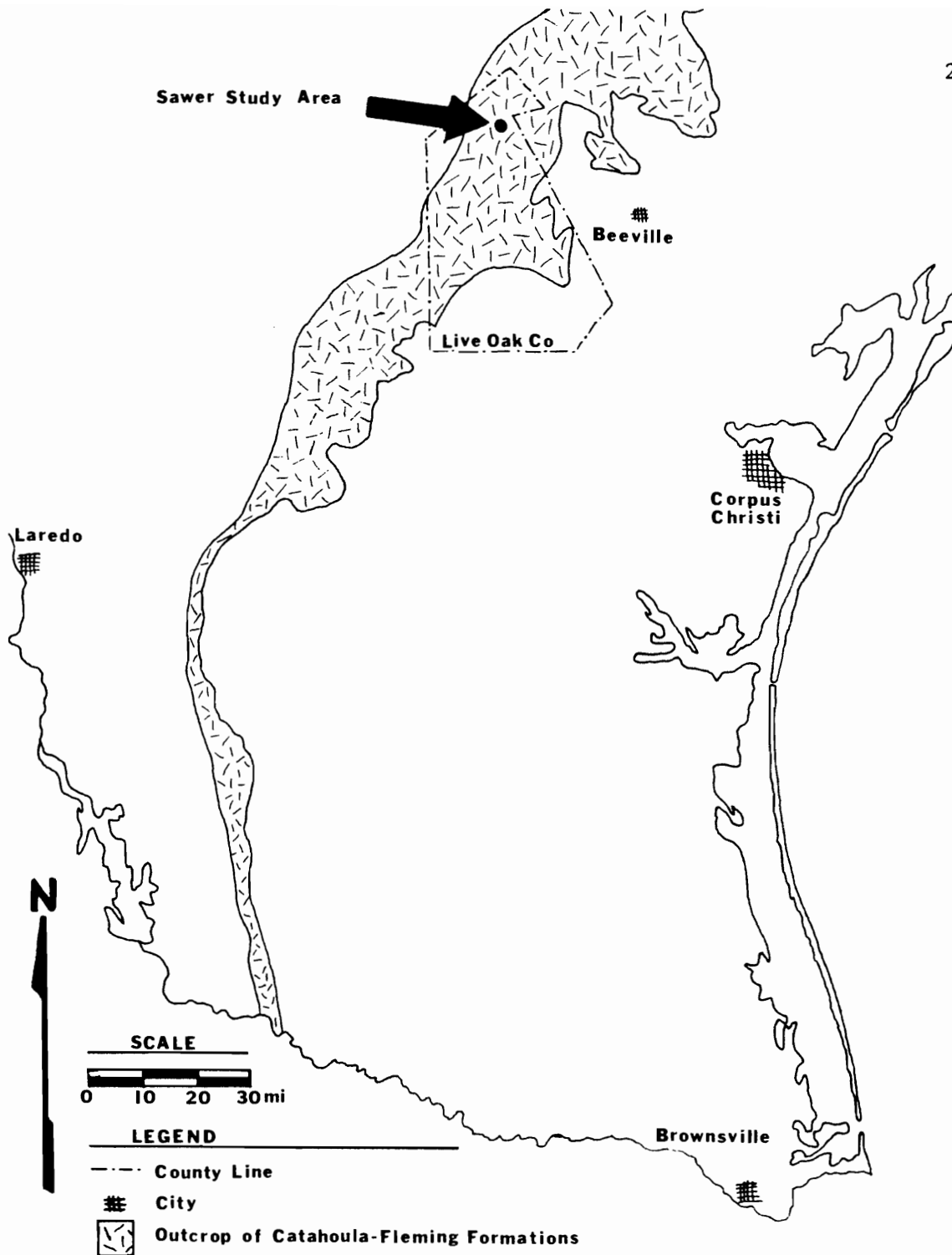


Figure 1. Location of the Sawyer Study Area in South Texas. (See Figures 2 and 3 for an enlargement of this area.) (After the AAPG Geological Highway Map of Texas, 1973).

several workers (Eargle and Weeks, 1961; Klohn and Pickens, 1970; Cathey, 1980). The details of an inorganic model for uranium mineralization stemmed from the sulfide petrology and sulfur isotope study of the south Texas Bruni deposit by Goldhaber et al. (1978). The model is termed inorganic because sulfate reducing bacteria are not directly necessary for the production of H_2S gas as a reductant. This H_2S gas, derived from deep-seated hydrocarbon accumulations, contains isotopically heavy sulfur that in turn enriches the sulfur component of the iron disulfides related to uranium mineralization. The isotopically heavy sulfur has been reported in the uranium-associated iron disulfides at the Bruni deposit by Goldhaber et al. (1978). As a result of that study, the inorganic, fault-derived reductant model has been widely applied to explain the reduction of several south Texas uranium deposits.

The biogenic model of uranium mineralization depends upon the activities of two types of bacteria, Thiobacillus for the oxidation of pre-ore pyrite and Desulfovibrio for the reduction of sulfate into H_2S gas. Inherent to the biogenic model is the presence of organic carbon within the host rocks to serve as a substrate for the sulfate-reducing bacteria. In addition to the presence of organic carbon, the biogenic model requires the availability of pre-ore stage pyrite (Busche et al., 1982). The biogenic formation of ore-associated H_2S reductant results in the isotopic enrichment of

light sulfur in the ore-stage iron disulfide minerals. Thus, uranium ore deposits genetically related to biogenic processes may be recognized by the presence of organic carbon, textures suggestive of relict organic structures and the characteristic light sulfur isotopic signature.

The purpose of this study is to describe the salient features of the Sawyer deposit and to interpret the origin and paragenesis of uranium-sulfide mineralization based upon these features.

CHAPTER II

SAMPLING AND ANALYTICAL TECHNIQUES

I. CORE SAMPLES

The Sawyer study is based upon the examination of seven mineralized borehole core sections along the strike of uranium mineralization (Figure 2). Cores were not available from the updip or downdip portions of the mineralization, thus the study is limited to the nose of the roll-front. The cores were supplied by the Sunoco Energy Development Company along with drill hole electric logs, base maps, core descriptions, uranium assays on foot-by-foot intervals and selected organic carbon analyses. Upon receipt, the cores were relogged and examined under a binocular microscope. From this examination, lithologic contacts were identified and compiled into a stratigraphic section.

The various core intervals which were selected for thin sections, polished thin sections, X-ray fluorescence, sulfur isotope analysis, electron microprobe and X-ray diffraction are illustrated in Figure 3. A total of 40 thin sections and 21 polished thin sections were prepared for studies of the host rock petrology and the opaque petrology. Trace element composition was determined through the X-ray fluorescence analysis of 20 samples. These samples were obtained by crushing a two inch interval of core centered on the drill hole footage depth selected for analysis. A similar method was used in extracting the 15 samples for sulfur isotope analysis. Sample intervals used for

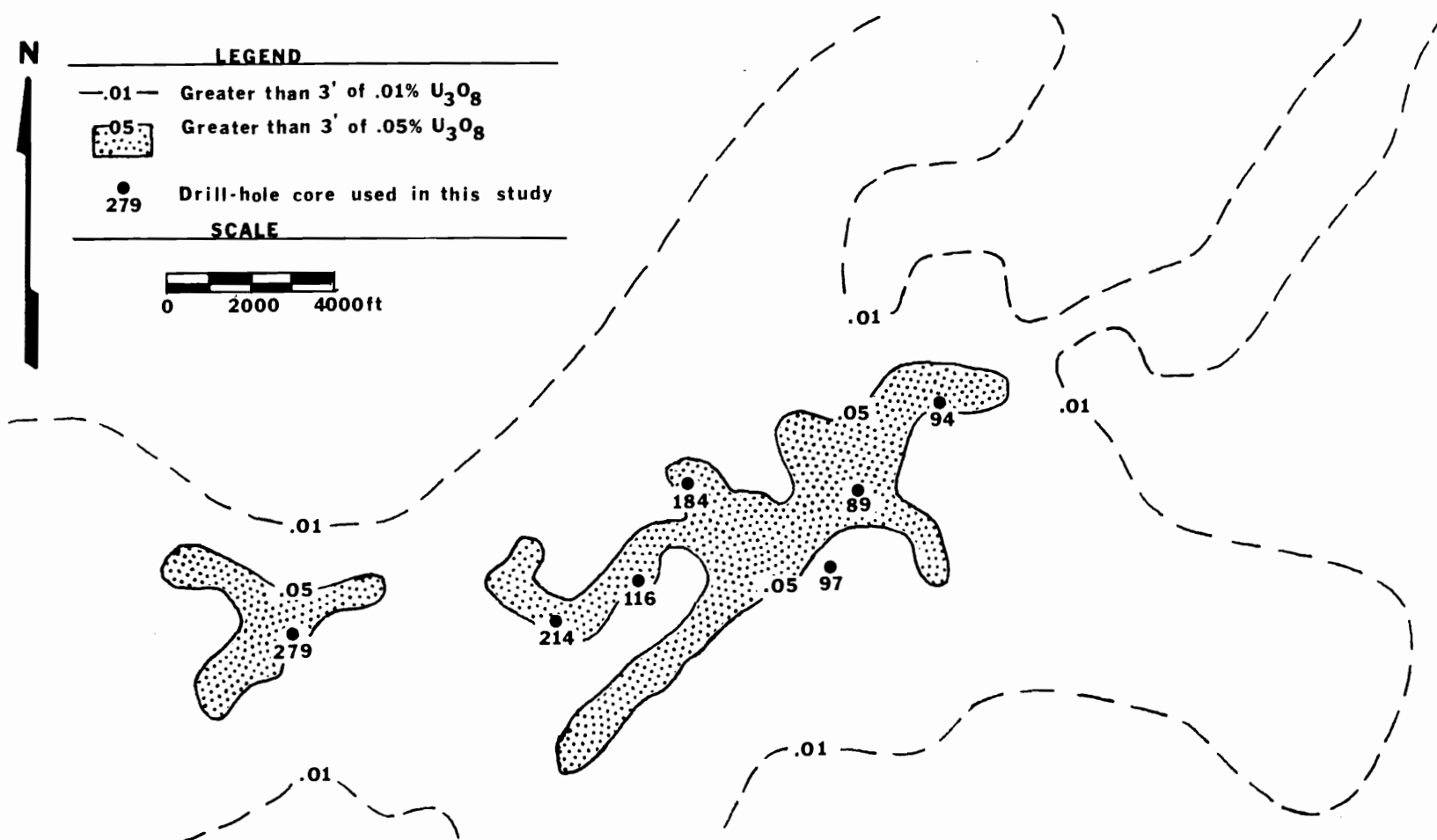


Figure 2. Sketch Map of the Sawyer Orebodies Showing the Location of Drill Holes Used in This Study.

X-ray diffraction (1), electron microprobe energy dispersion analysis (1), and SEM (5) are also shown in Figure 3.

II. ANALYTICAL TECHNIQUES

Host Rock Petrology

Modal analysis of the thin sections was based on point counting 400 grains per thin section, with a 30 μ counting interval. A Swift stage, coupled with a mechanical counter, was used to maintain the proper interval and tabulate the results.

Opaque Petrology

The opaque mineralogy and textures were studied through the use of standard reflected light microscopic examination of polished thin sections.

Scanning Electron Microscopy

Samples for SEM examination were extracted by cutting small sections from the cores, mounting these on a SEM stage and gold-coating them for electrical conductivity. The identification of uranium-enriched phases was made through energy dispersion analysis and the resulting spectra were reproduced on an X-Y plotter. Scanning electron microscopy was conducted at The University of Tennessee Department of Metallurgical Engineering.

X-Ray Fluorescence Analysis

Samples were initially qualitatively analyzed for trace elements at the facilities of Oak Ridge Associated Universities, Oak Ridge, Tennessee. Quantitative analyses of the identified trace elements were done through X-ray Assay Laboratories Limited, Don Mills, Ontario, Canada. The trace constituents which were analyzed included Mo, Zn, As, Rb, Sr, Pb, MnO, Fe_2O_3 , Y, and TiO_2 .

Uranium and Organic Carbon

Uranium and organic carbon analyses were conducted by Core Laboratories, Inc., Corpus Christi, Texas. Uranium concentrations were determined through wet chemical techniques. Organic carbon was digested in wet dichromite solution, absorbed onto Ascarlite, dried and weighed to determine weight percentage (Jackson, 1982, personal communication). Analytical error in this procedure is reported to be $\pm 0.5\%$. These uranium and organic carbon results were provided by the Sunoco Energy Development Company.

Sulfur Isotope Analysis

Samples for sulfur isotope analysis were selected from core intervals within the ore mineralized zones and the unmineralized horizons above and below the ore. Each sample was ground into -100 mesh powder and analyzed at the stable isotope lab of Indiana University at Bloomington. Sulfur was extracted from the powdered samples by boiling in Thode solution to produce H_2S . This H_2S was then combined with cadmium acetate to form CdS which was subsequently added to AgNO_3 ,

to form Ag_2S . The excellent burning properties of silver sulfide produced SO_2 , which allowed the isotopic composition to be determined spectrographically (Ripley, 1982, personal communication). Analytical sulfur isotope values represent bulk sulfide samples, as no effort was made to separate pyrite from marcasite; however, more than 95% of the sulfides are in the form of marcasite, as determined by optical examination.

X-Ray Diffraction

Loosely consolidated ore material, from the strongly mineralized interval at 522 feet in core 279, was selected for X-ray diffraction analysis to detect possible uranium minerals. The sample was mounted in an epoxy slug, then attached to X-ray film for a one week exposure time, resulting in an autoradiograph. Radioactive areas of the slug were then extracted and examined under a binocular microscope. Several very fine, dark grains were removed and mounted in a Gandolfi camera. The samples were X-rayed for 7-1/2 hour and 24 hour exposures.

Electron Microprobe Energy Dispersion Analysis

A black, sooty, unidentifiable phase was noted in the core descriptions and appeared to correlate with intervals of higher uranium concentrations. A sample of this material was mounted in an epoxy slug and polished to a smooth surface. The slug was then placed under the electron microprobe beam and four separate areas were analyzed for identifiable peaks using the energy dispersion mode.

CHAPTER III

GEOLOGIC SETTING

I. REGIONAL GEOLOGY

Catahoula Depositional Systems

The Catahoula Formation of the Texas Coastal Plain south of the San Marcos Arch comprises sediments deposited by the Gueydan fluvial system (Galloway, 1977). The Gueydan depositional system is represented by bed-load, channel-fill and crevasse-splay fluvial facies surrounded by tuffaceous siltstone, mudstone and claystone facies of floodplain and lacustrine origin. Gueydan sediments were supplied by a single large river system originating in west Texas (Galloway, 1977) and from wind-fall volcanic ash derived from extensive Oligocene volcanism in west Texas and northeastern Mexico (McBride et al., 1968).

Structural Development

The Texas Coastal Plain is affected by strike-oriented, tensional growth faults and intrusive diapiric structures. Growth fault development is directly related to the history of sediment loading in the actively subsiding Gulf Coast basin (Fisher, 1973; Jones and Wallace, 1974; Dailly, 1976). Conditions leading to growth faulting and diapirism were initiated by the deposition of thick, undercompacted, slope and prodelta mud sequences. Tectonic subsidence and burial of these muds leads to overpressurization in the sediments. This results in plastic, lateral bedding plane slippage and upward mobilization of

mud and salt diapirs. The deep bedding plane slippage requires a compensating response in the overlying sediment pile. This response is the formation of basinward-displaced growth faults and associated antithetic faults, with displacements ranging from a few hundred feet near the surface to several thousand feet in the subsurface. Upward-mobilized masses of mud and salt give rise to the formation of diapirs and diapir-related fault structures. Growth faulting was active during Catahoula deposition and locally exerted a pronounced influence on the pattern of sedimentation (Galloway, 1977).

II. LOCAL GEOLOGIC SETTING

Stratigraphy

The Sawyer deposit is hosted within the basal Catahoula sediments in northeastern Live Oak County. The host sediments were deposited in a transition zone between a major strike-parallel fluvial axis that transects northeastern Live Oak County (Figure 4) and lacustrine ash, silt and mud facies to the south (Galloway, 1977). Correlation of Sawyer drill hole core lithologies and electric logs indicates that the host sediments represent a fluvial crevasse-splay facies (Figure 5). Detailed correlation suggests that an early crevasse-splay channel was scoured and partially removed by the deposition of a second crevasse-splay channel. Individual channel sequences are 15 to 40 feet (4.6 to 12.2 m) in thickness and about one mile (1.6 km) in width. The crevasse-splay channels were developed during the flood stage breaching of the major fluvial axis in northern Live Oak County. Downdip from the Sawyer

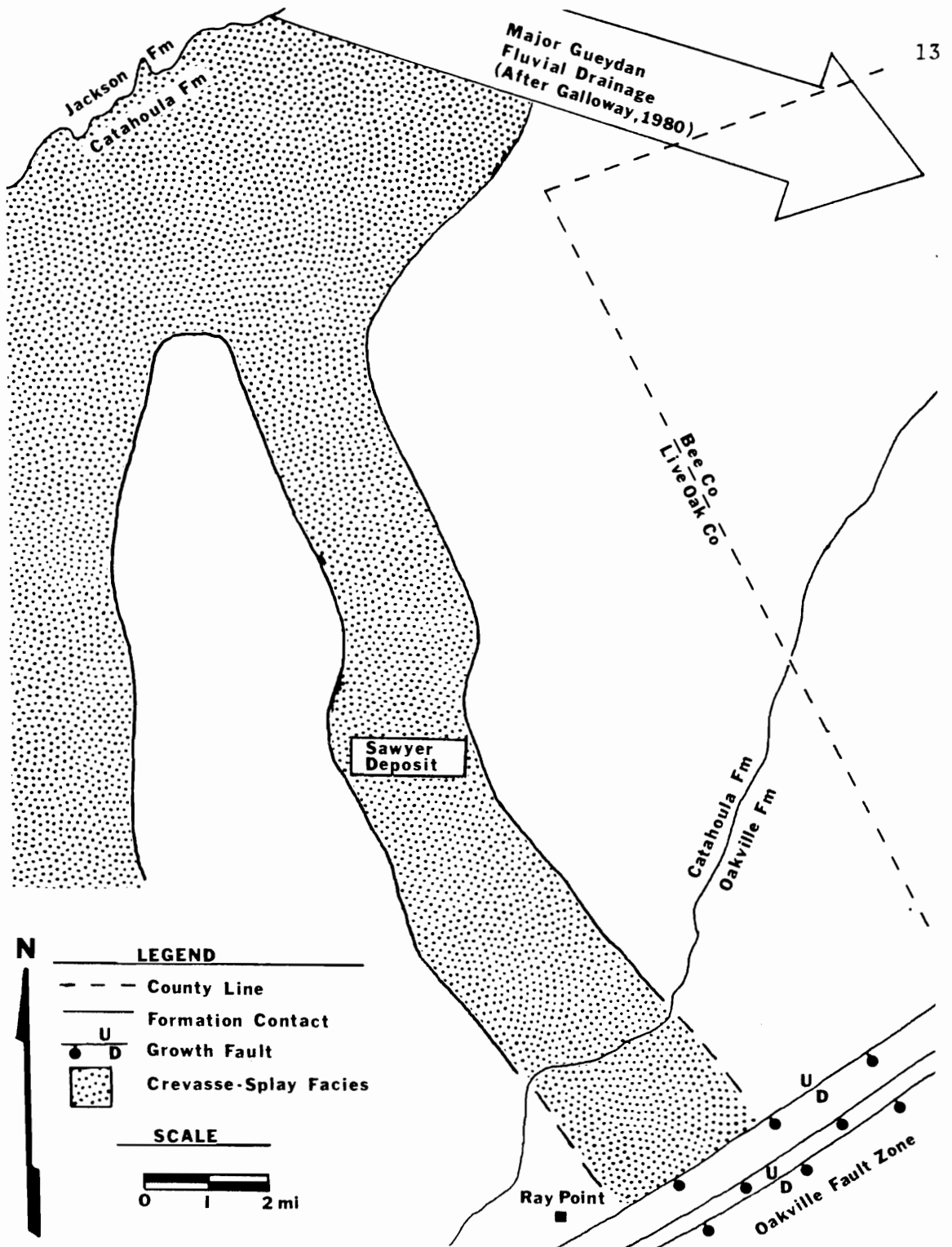


Figure 4. Geologic Map of the Sawyer Area in Northeastern Live Oak County Showing Facies Distribution in the Catahoula Formation.

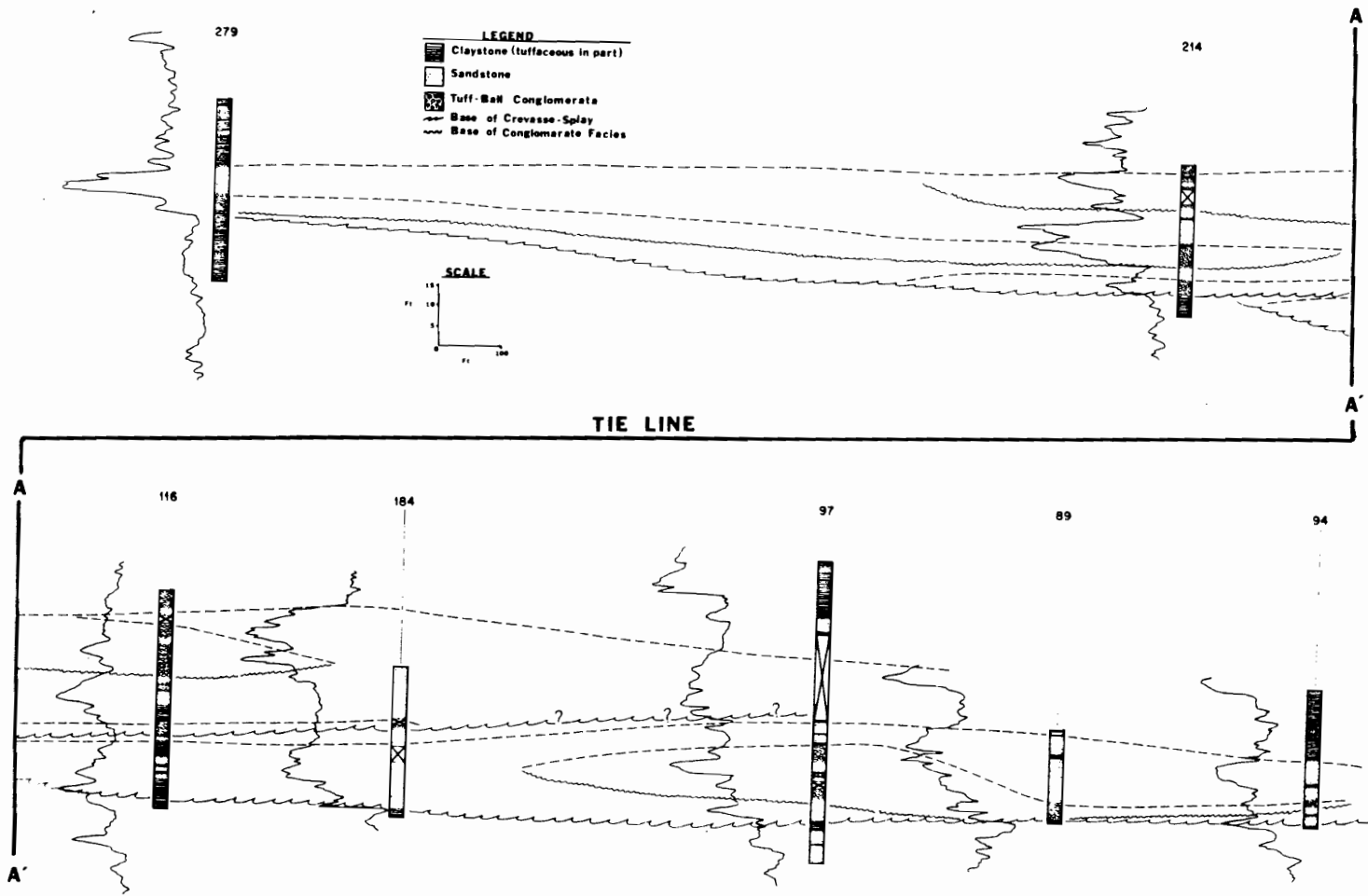


Figure 5. Lithologic and SP Log Correlations Across the Sawyer Core Holes Used in This Study.

prospect, the crevasse-splay sediments fed prograding lacustrine deltas, which interfinger with the lacustrine facies of Galloway (1977).

Crevasse-Splay Lithofacies

Distinct crevasse-splay lithofacies displaying a crude, fining-upward sequence are developed in the Sawyer area. The basal channel facies is composed of tuff-ball conglomerate with a medium-grained, subangular sand matrix. Tuff-ball conglomerates range from 2 to 8 feet in thickness and grade upward into sand. These sands are tuffaceous, subangular, fine- to medium-grained, with abundant volcanic debris and varying amounts of diagenetic clay. Sand lithofacies are overlain by fine-grained, tuffaceous floodplain silt and clay. The floodplain facies contain distinct paleosol horizons that may have been augmented by the direct addition of airfall ash. A more complete account of these lithologies will be given in a later section.

Structure

The Sawyer prospect is located approximately six miles updip from the Oakville Fault Zone, a belt of clustered growth faults that transect central Live Oak County. The Oakville Fault Zone is well known for the prolific oil and gas fields associated with it. Extensive drill hole data indicate that faults are not present in the Sawyer area and that the Catahoula dips gently from 2° to 5° southeastward.

CHAPTER IV

HOST ROCKS

I. PETROLOGY

Tuff-Ball Conglomerate

The tuff-ball conglomerate which occurs at the base of the crevasse-splay sequences consists of abundant, rounded tuff clasts with interstitial, medium to fine sand grains within a clay matrix and calcite cement. Proximal to ore mineralization, the conglomerate contains substantial concentrations of amorphous black, sooty minerals containing Mg, Fe, Mo, S, K, Na, Si, Al, and Ca as revealed through electron microprobe energy dispersion analysis. Individual tuff-ball clasts range from one-fourth to three inches (0.6 to 7.5 cm) in diameter and are composed of glass shards, quartz, feldspar and micrite fragments incorporated into a clay matrix (Figure 6A). Interstitial sand grains comprise quartz, feldspar, micrite, ilmenite and sand-sized volcanic rock fragments. Diagenetic features include argillized glass shards, clay rims (cutans) surrounding detrital grains, calcite cement and grain replacement, and authigenic zeolites and sulfides. Modal analysis of two representative tuff-ball conglomerate samples is shown in Table 1.

Sandstone

The sandstone lithologies represent a fining-upward facies overlying the tuff-ball conglomerate and are comprised of tuffaceous,

Figure 6. Photomicrographs of Thin-Sections in Transmitted Light.
(All photomicrographs are at the same scale.)

- A. Sample 279-521. Tuff-ball conglomerate showing tuff-balls surrounded by calcite cement.
- B. Sample 279-525. Paleosoil horizon displaying root tubules and abundant, opaque, fine-grained sulfides.
- C. Sample 214-508. Fine-grained sandstone with argillized glass shards (crossed nicols).
- D. Sample 116-491. Tuff-ball conglomerate displaying pedogenic clay cutans as highly birefringent rims (crossed nicols).

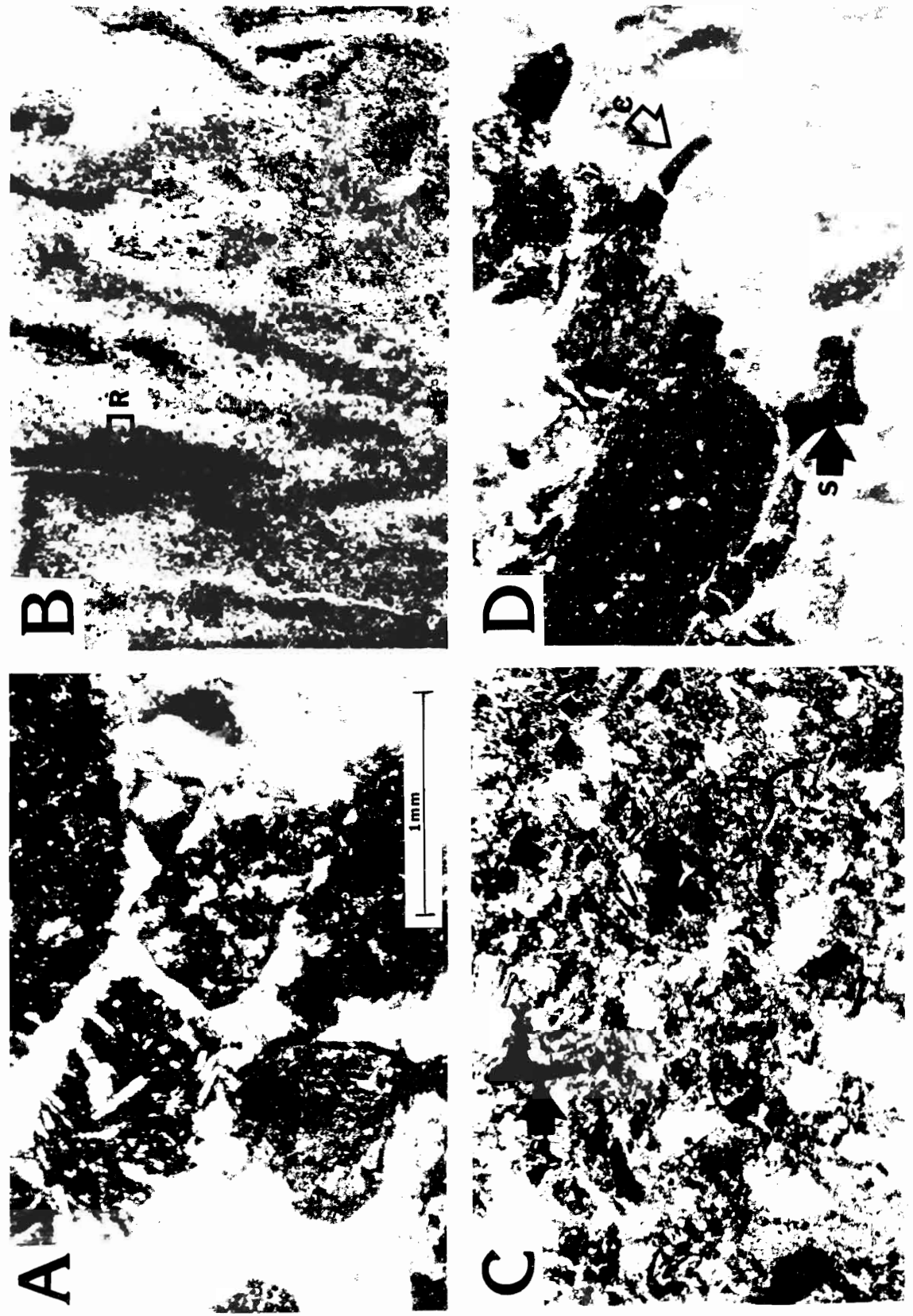


Figure 6

Table 1. Modal Compositions of the Sawyer Lithologies Given in Percent.

Number of Samples	Lithology	Tuff- Ball	Quartz	Plag. Feldspar	Micrite Nodule	Glass Shard	Volcanic		Clay Matrix	Clay Cutan	Zeolite	Opaque	Other
							Rock Fragment	Calcite Cement					
2	Tuff-Ball Conglomerate	79	1	tr	2	3	4	5	4	tr	tr	1	1
2	Sandstone	--	22	2	tr	3	29	20	9	tr	2	9	4
3	Claystone	--	6	tr	tr	20	tr	3	60	4	tr	6	1

very fine- to medium-grained, subangular to subrounded sand, with variable amounts of matrix and calcite cement. The matrix includes diagenetic clay cutans surrounding detrital grains, argillized glass shards, squashed volcanic rock fragments and authigenic clay, zeolites and sulfides. Calcite cement is ubiquitously present in various amounts and locally replaces framework and diagenetic constituents. Modal analysis of two representative sandstone samples is shown in Table 1.

Claystone

Claystones representing overbank facies and paleosoil horizons are comprised of clay matrix and argillized shards, with variable amounts of very fine-grained quartz, volcanic rock fragments, feldspars, opaques and patchy calcite cement. Many of the claystones are thoroughly altered air-fall tuffs and overbank floodplain accumulations. The average of the modal analyses of three claystones is also presented in Table 1.

Classification

The compositions of the tuff-ball conglomerate, sandstone and claystone are plotted in Figure 7 using Folk's (1974) classification. The compositions occupy the extreme feldspar-depleted edge of the litharenite field. However, this position in the litharenite field may not be representative of the original depositional composition of these sediments because core intervals selected for this study were recovered only from zones in, or near, uranium mineralization. Corrosive, ore-stage fluids may have removed much of the original feldspar, thus

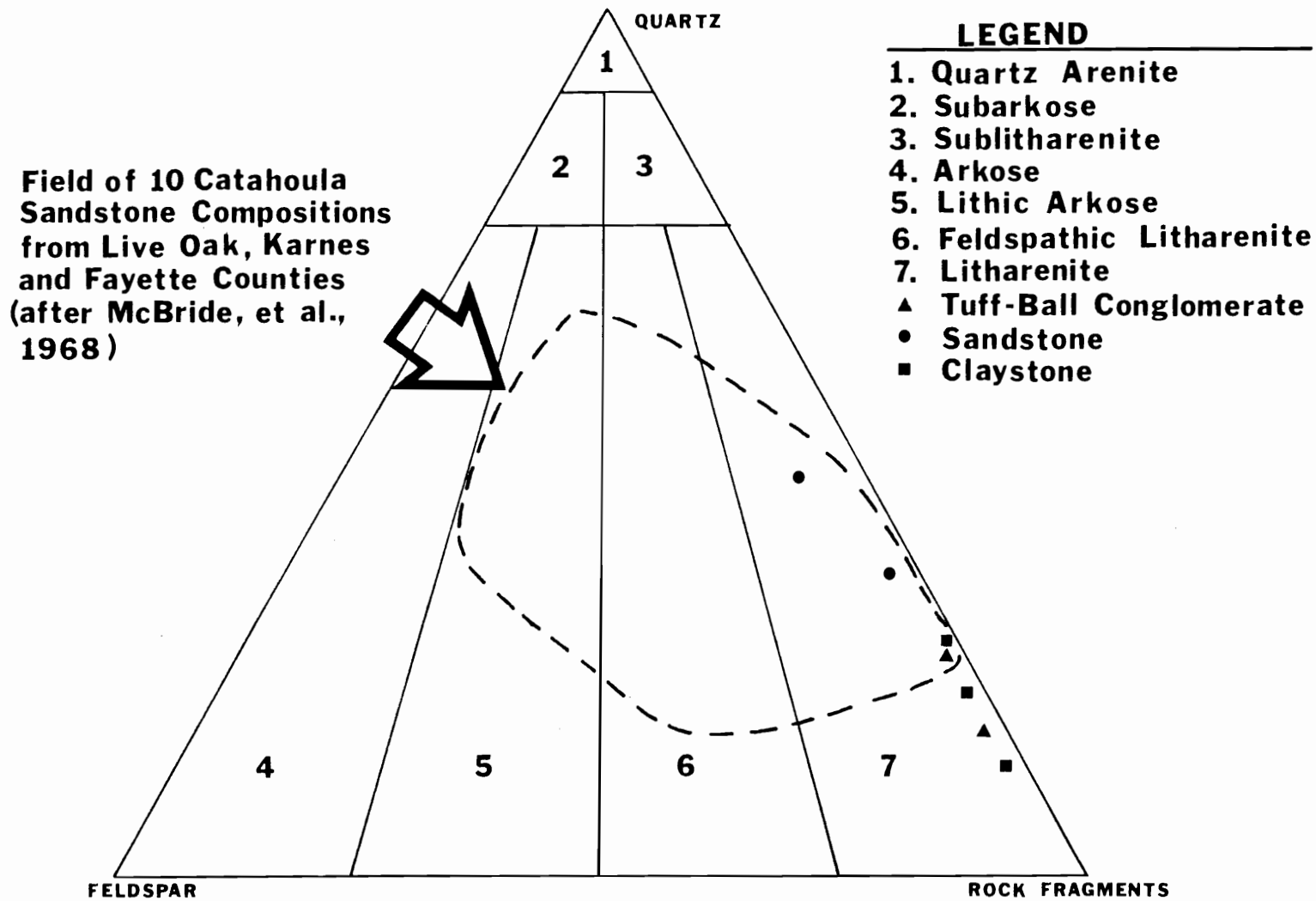


Figure 7. QFR Compositions of Sawyer Lithologies According to Folk's (1974) Classification Scheme.

resulting in an artificial skew to the present composition. The embayed, corroded and altered appearance of much of the feldspar observed in the core samples supports this interpretation.

Interpretation

The composition and nature of the tuff-ball conglomerate, sandstone and claystone may be explained as products of deposition in a crevasse-splay, fluvial environment. The tuff-ball conglomerate is considered to be equivalent to the lumpy, pisolitic tuff of McBride et al. (1968). The conglomerates are interpreted to result from the agglomeration of loose, surficial ash and soil materials during rain and flood. The tuff balls accreted as they were rolled into crevasse-splay channels and subsequently were transported as bed load for relatively short distances. This transport mechanism is supported by the erosion-scoured contact between the tuff-ball conglomerate and the underlying sediment. The tuff-ball conglomerate grades upward into medium- to fine-grained sand, representing a fining-upward trend similar to that described by Coleman (1969) for crevasse-splay sediments associated with the Brahmaputra River in India. As crevasse-splay velocities decreased, fine-grained overbank silt and clay were deposited to envelop the channel sediments. Following a flood event, soil horizons developed on the fine-grained facies (Figure 6B, page 18), incorporating direct additions of windfall-derived volcanic ash.

II. DIAGENESIS

Diagenetic Features

Catahoula sediments display syngenetic to very early postdepositional, open hydrologic system, diagenetic products (Galloway and Kaiser, 1980). Diagenetic features and products have been examined from the study of petrographic thin sections and with the use of scanning electron microscope techniques. Diagenetic products include pedogenic clay cutans, diffuse to discrete micrite nodules, argillation of glass shards, authigenic sulfides, clay booklets, zeolites and calcite cement (Figure 6C, page 18). Clay cutans rimming detrital grains are locally well developed and are easily diagnosed by their high birefringence (Figure 6D, page 18). Authigenic sulfides are common to abundant and display a preference for intergranular (open space) sites, or selective replacement in volcanic rock fragments, tuff clasts and micrite nodules.

Timing of Diagenesis

Petrologic examination of the Sawyer lithologies suggests a diagenetic sequence as follows:

1. Deposition of sediments in a crevasse-splay channel along the margin of a major, strike-oriented fluvial system in northern Live Oak County.
2. Moderate pedogenic weathering of subaerially exposed sediments, producing clay cutans, micrite nodules and minor argillation of the glass shards.

3. Uranium mineralization and sulfidization of the sediments.
4. Precipitation of most of the sparry calcite cement as grain replacement and pore fill.
5. Open-hydrologic system diagenesis, including the argillation of glass shards and precipitation of zeolites.
6. The development of late-stage calcite cement to greatly reduce the remaining porosity.

The composition and nature of the diagenetic constituents, along with their textural relationships, are consistent with those produced during the pedogenesis and very early diagenesis of volcanoclastic sediments. Following the early diagenesis of the sediments, late-stage calcite cement was precipitated to fill nearly all of the available pore space, resulting in a system which has remained stagnant since diagenesis. The diagenetic sequence described above is similar to that described by Galloway and Kaiser (1980) for the nearby, Catahoula-hosted, House-Seale deposit.

CHAPTER V

URANIUM MINERALIZATION

I. URANIUM DISTRIBUTION

Uranium occurs throughout the crevasse-splay channel sediments, with the richest accumulations (0.1% to 0.943% U_3O_8) concentrated in the tuff-ball conglomerates and the adjacent, underlying claystones found at the base of the channel sequences. Within these crevasse-splay sediments, discrete uranium mineralization fronts have been delineated through exploratory drilling in the Sawyer area. The approximate aerial extent of two trends of 0.01% U_3O_8 mineralization is shown in Figure 8. Higher grade uranium mineralization (greater than 3' of 0.05% U_3O_8) occurs as pods within these lower grade mineralization trends. Each mineralization trend represents the position of a former redox interface along which uranium and associated trace elements were precipitated. The Sawyer deposit described in this study is one of the larger pods discovered along these mineralization fronts. The distribution of uranium assays in the Sawyer cores is illustrated in Figure 9.

II. ASSOCIATED TRACE ELEMENTS

The results of trace element analyses are presented in Table 2. Trace element correlations were obtained using computer-generated Pearson correlation coefficients and are presented in Table 3. Uranium

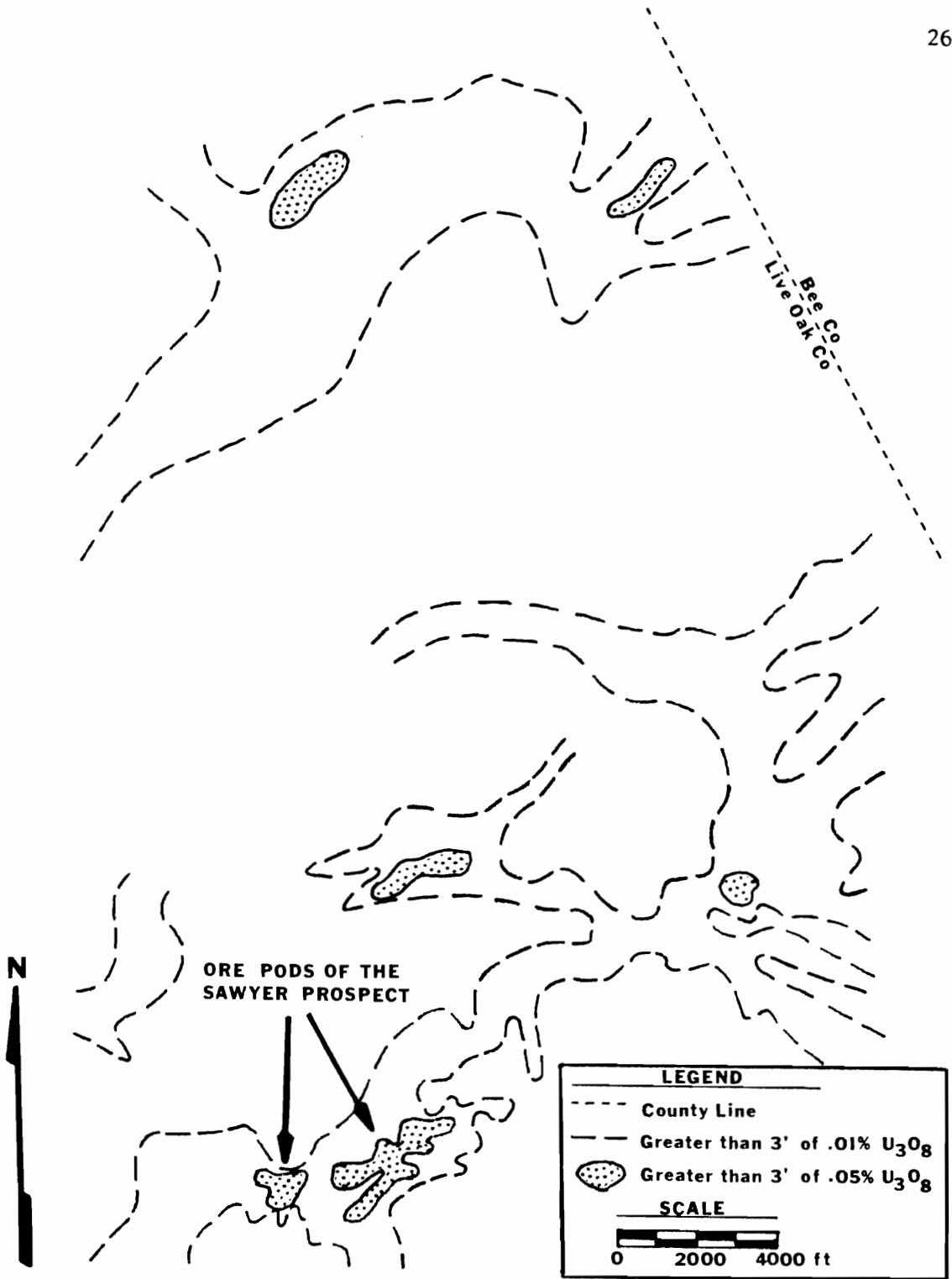
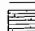


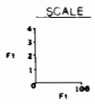


Figure 8. The Distribution of Catahoula Uranium Mineralization Fronts in Northeastern Live Oak County.

279

LEGEND

-  Claystone (tuffaceous in part)
-  Sandstone
-  Tuff-Ball Conglomerate



214

116

184

97

89

94

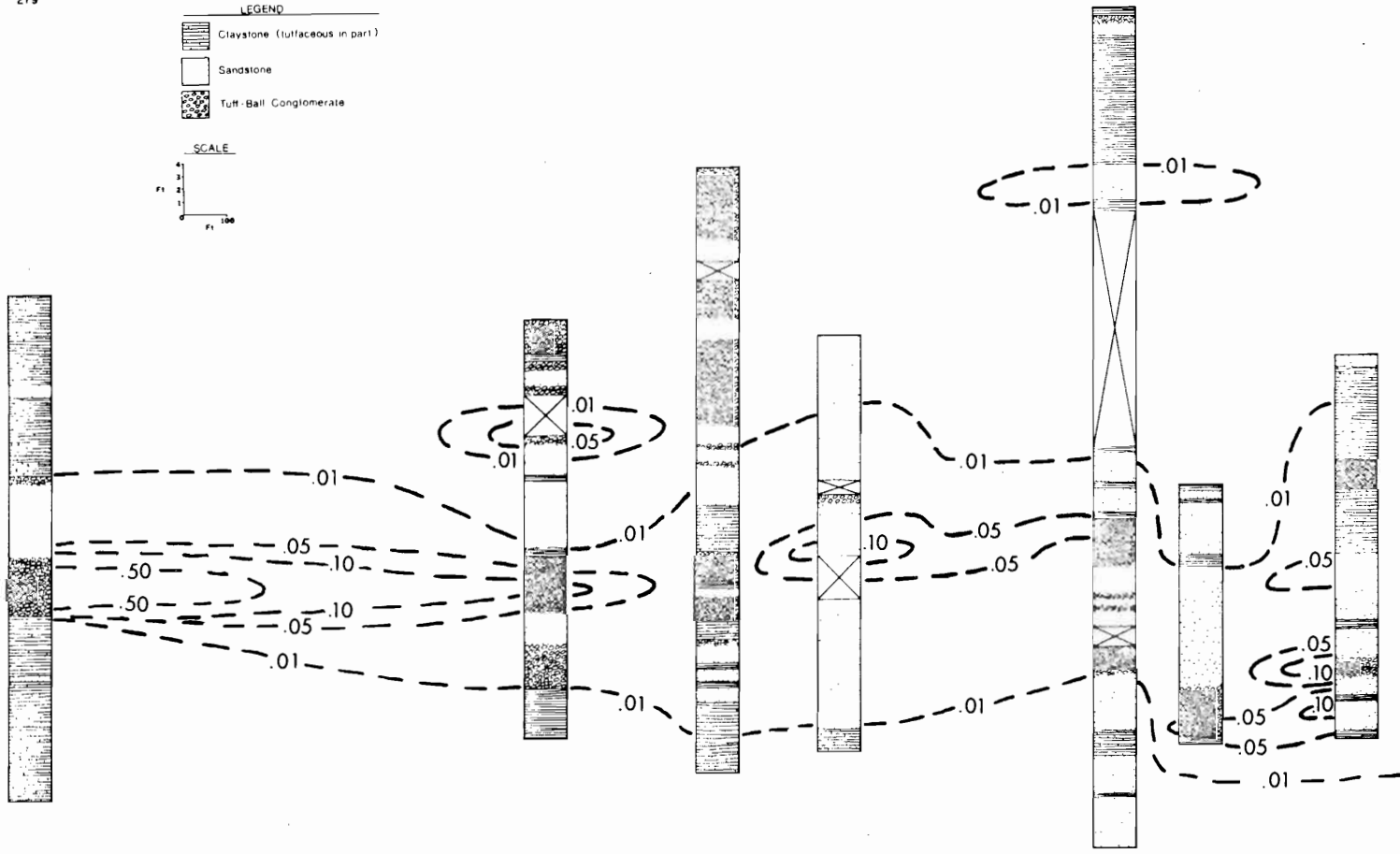


Figure 9. The Distribution of Uranium Mineralization Across the Sawyer Cores Expressed as Chemical Percentage.

Table 2. Uranium and Associated Trace Element Concentrations. Fe₂O₃ and MnO are given as weight percent; all other data are presented as ppm.

Sample	U ₃ O ₈	Mo	Zn	As	Rb	Sr	Zr	Pb	MnO	Fe ₂ O ₃	Y	TiO ₂
279-505	50	18	79	18	130	170	200	22	0.04	2.52	40	0.41
279-515	290	11	54	12	90	280	250	22	0.06	1.95	30	0.61
279-517	170	15	44	12	60	370	280	30	0.08	1.70	50	0.70
279-519	2020	4000	100	940	220	220	200	65	0.07	3.67	100	0.26
279-521	9430	770	53	320	260	200	210	86	0.06	3.82	90	0.69
279-523	170	240	47	130	80	290	120	33	0.07	2.68	10	0.43
279-525	60	24	80	20	130	140	160	23	0.03	4.71	10	0.53
214-485	50	16	63	15	110	250	250	24	0.04	2.19	50	0.43
214-502	550	10	62	17	80	260	280	20	0.05	2.06	50	0.48
214-508	230	600	63	85	60	370	140	38	0.08	1.86	40	0.31
116-490	90	21	77	23	120	180	190	26	0.04	2.39	30	0.28
116-517	160	130	56	67	100	350	280	18	0.03	2.79	40	0.63
116-522	160	140	76	37	130	160	220	24	0.06	2.95	30	0.28
116-530	200	56	61	24	10	160	60	50	0.11	1.41	40	0.21
116-535	180	19	75	15	90	350	230	24	0.04	3.17	50	0.70
97-490	20	2.5	79	13	130	190	220	18	0.03	2.72	40	0.47
97-520	110	97	63	38	130	260	240	12	0.03	2.92	30	0.46
97-530	190	30	78	35	140	180	220	18	0.08	2.26	50	0.38
97-535	70	62	37	22	40	260	70	42	0.12	1.11	40	0.19
97-545	30	11	75	19	100	250	220	20	0.06	2.84	30	0.49

Table 3. Pearson Correlation Coefficients for the Sawyer Trace Element Data Presented in Table 2.

U ₃ O ₈	1.00											
	0.00											
Mo	0.31	1.00										
	0.17	0.00										
Zn	-0.11	0.46	1.00									
	0.65	0.04	0.00									
As	0.44	0.99	0.41	1.00								
	0.05	0.00	0.07	0.00								
Rb	0.70	0.53	0.48	0.62	1.00							
	0.00	0.02	0.03	0.00	0.00							
Sr	-0.14	-0.04	-0.49	-0.07	-0.37	1.00						
	0.55	0.87	0.03	0.76	0.11	0.00						
Zr	0.04	-0.05	0.15	-0.04	0.33	0.28	1.00					
	0.86	0.83	0.53	0.87	0.16	0.24	0.00					
Pb	0.79	0.59	-0.12	0.66	0.41	-0.07	-0.36	1.00				
	0.00	0.01	0.61	0.00	0.07	0.78	0.12	0.00				
MnO	0.34	0.13	-0.41	0.12	-0.40	0.06	-0.64	0.48	1.00			
	0.88	0.57	0.07	0.63	0.08	0.80	0.00	0.03	0.00			
Fe ₂ O ₃	0.38	0.34	0.54	0.40	0.73	-0.31	0.21	0.07	-0.60	1.00		
	0.10	0.15	0.01	0.08	0.00	0.18	0.38	0.76	0.01	0.00		
Y	0.62	0.66	0.25	0.68	0.56	-0.09	0.09	0.72	0.24	0.10	1.00	
	0.00	0.00	0.29	0.00	0.01	0.69	0.71	0.00	0.31	0.69	0.00	
TiO ₂	-0.06	-0.05	-0.16	-0.03	-0.04	0.34	0.29	-0.16	-0.26	0.06	-0.38	1.00
	0.80	0.84	0.51	0.90	0.85	0.14	0.22	0.51	0.26	0.81	0.10	0.00
	U ₃ O ₈	Mo	Zn	As	Rb	Sr	Zr	Pb	MnO	Fe ₂ O ₃	Y	TiO ₂

concentrations are seen to correlate with the presence of As (Figure 10), Rb (Figure 11), Pb (Figure 12) and Y (Figure 13).

III. ORGANIC CARBON

Organic carbon content was analyzed at one foot intervals within the strongly mineralized portion of core 279 and at irregular intervals within core 214. Although the values are uniformly low (less than 0.28%), they are significant in that organic carbon is often below detection limits (0.01%) in many of the Catahoula orebodies (Galloway and Kaiser, 1980). A Pearson correlation coefficient of 0.286 between organic carbon and uranium, with a confidence of 0.125, suggests that there is no strong statistical correlation between organic carbon and uranium (Figure 14).

IV. ORE MINERALOGY

Uranium Mineralogy

The nature of the uranium mineralization was investigated through the use of a scanning electron microscope (SEM), with energy dispersive capability, and X-ray diffraction techniques. Uranium-enriched areas, located in an SEM sample, were found to occur as scaly encrustations on the surfaces of sand grains (Figure 15A). An energy dispersion spectrum, obtained from the encrustation illustrated in Figure 15B, revealed the presence of U, Al, Si, K, Fe, Ca and S (Figure 16). The appearance and composition of these encrustations suggest that they are an amorphous phase of uranium which has adsorbed onto favorable mineral surfaces.

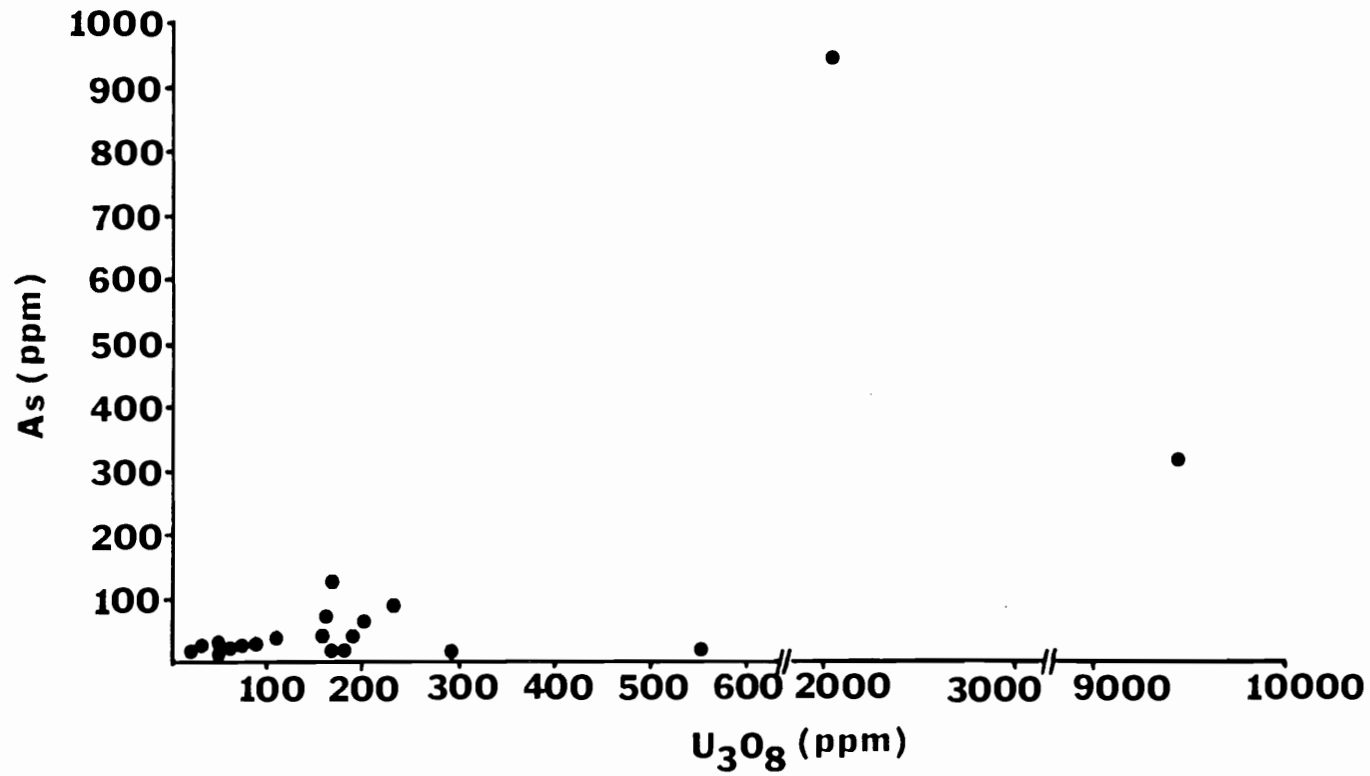


Figure 10. Plot of U₃O₈ vs. As Concentrations in 20 Sawyer Core Samples.

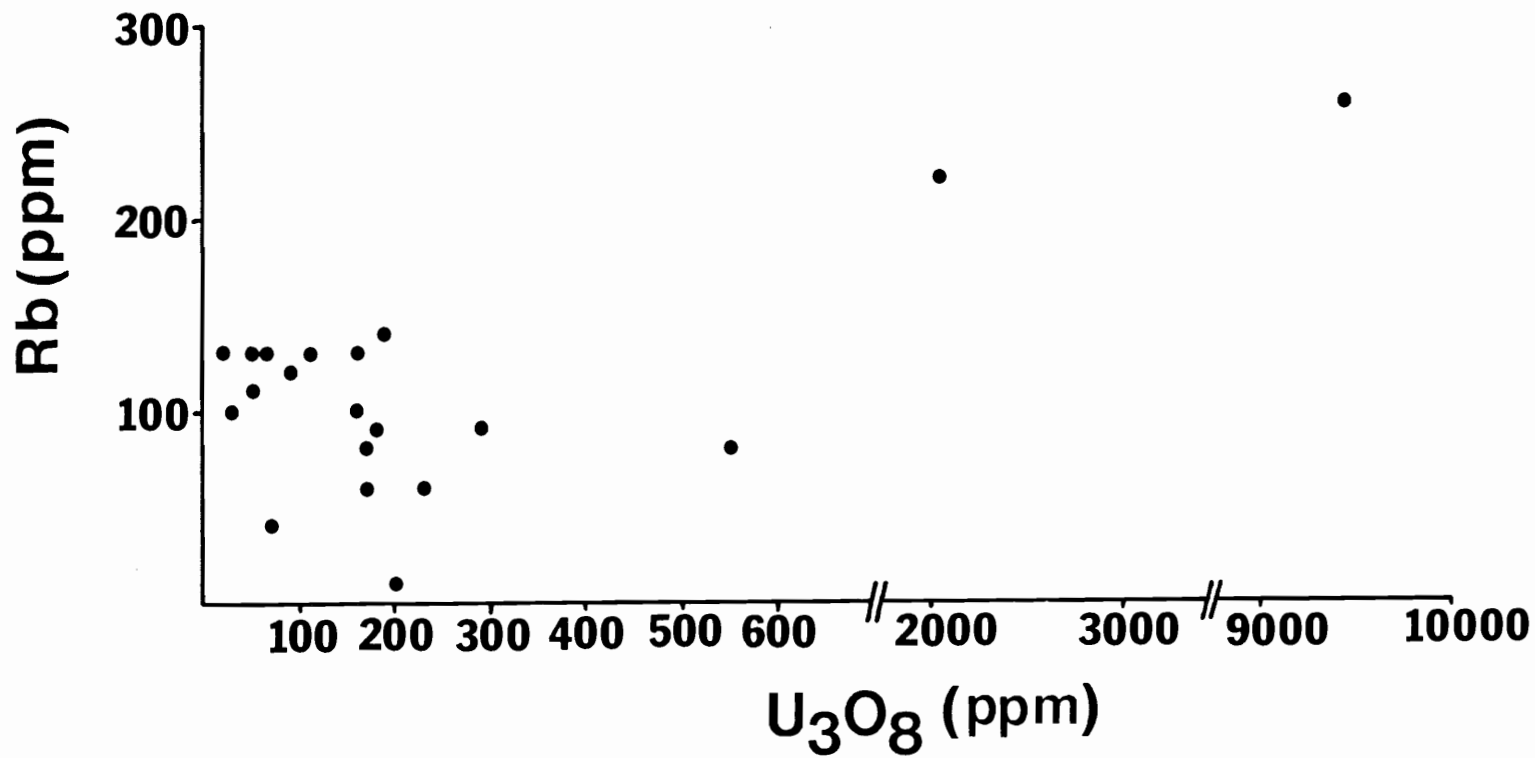


Figure 11. Plot of U₃O₈ vs. Rb Concentrations in 20 Sawyer Core Samples.

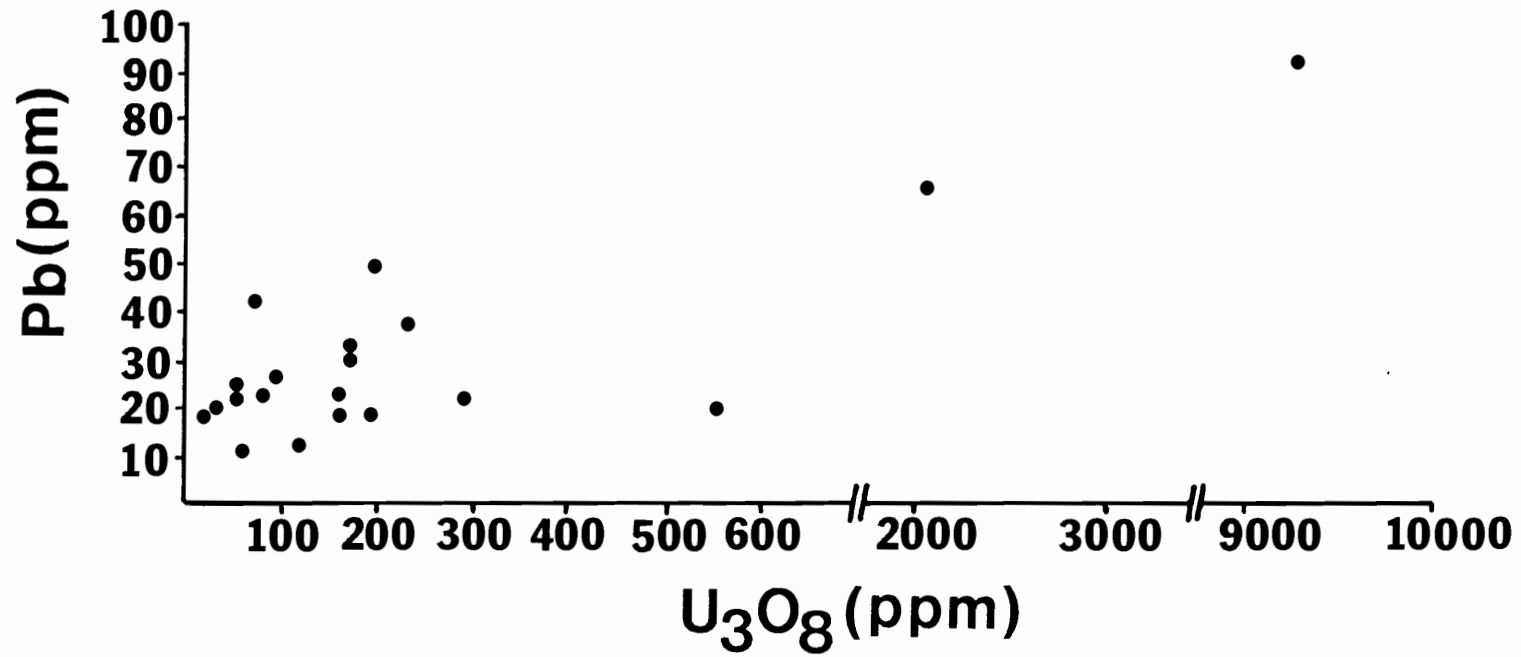


Figure 12. Plot of U_3O_8 vs. Pb Concentrations in 20 Sawyer Core Samples.

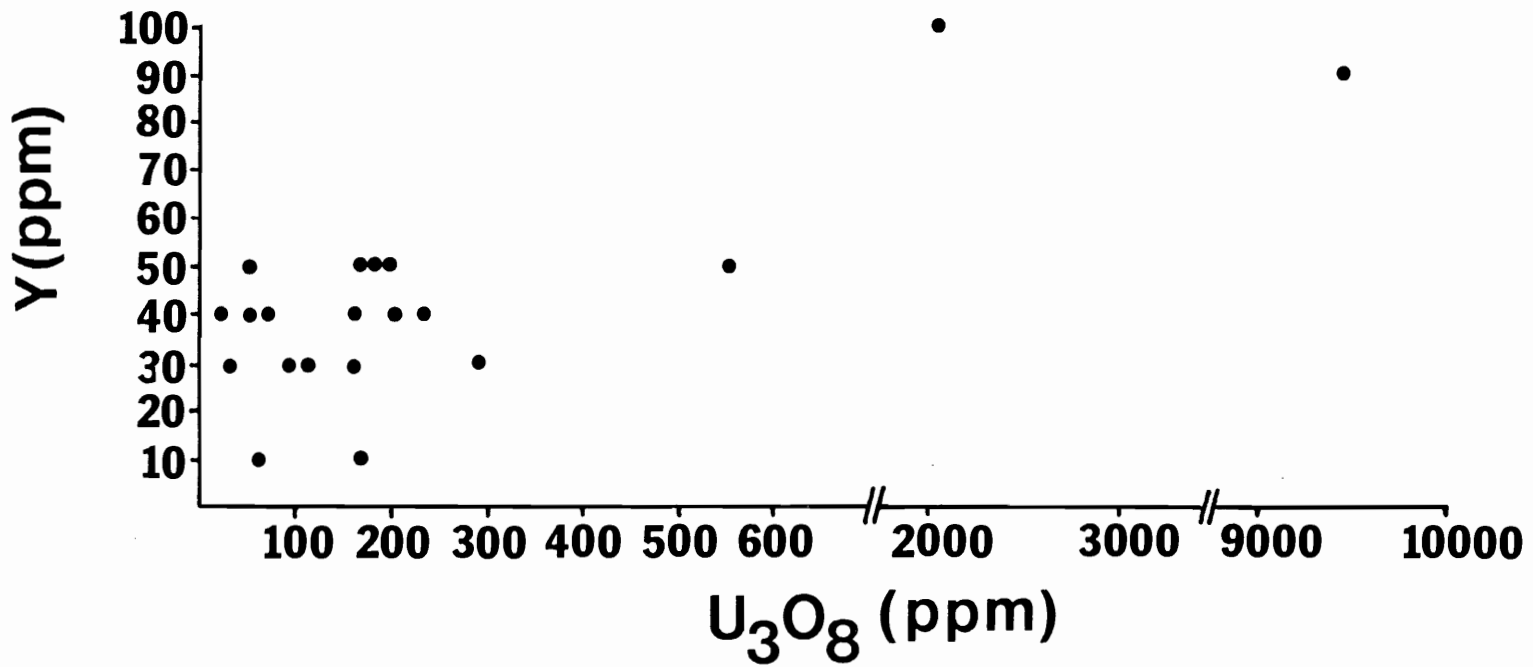


Figure 13. Plot of U_3O_8 vs. Y Concentrations in 20 Sawyer Core Samples.

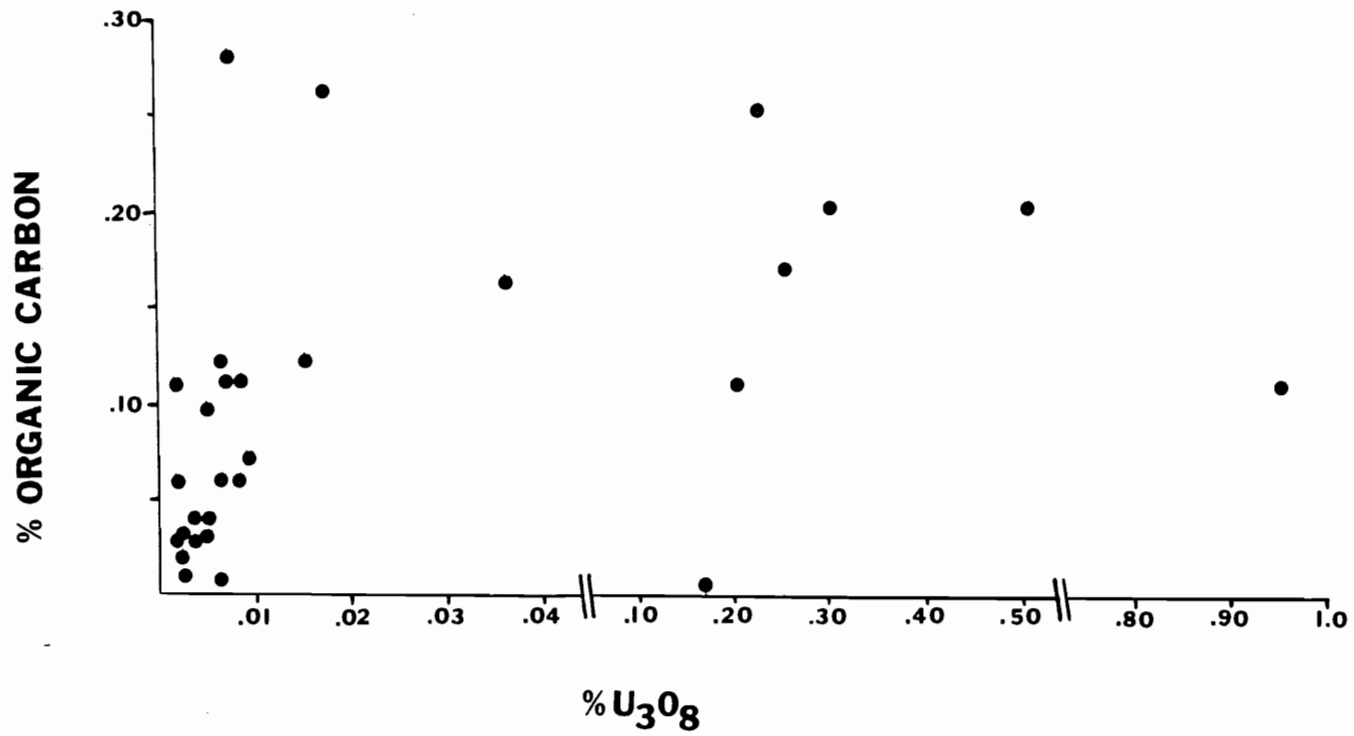


Figure 14. Plot of U₃O₈ vs. Organic Carbon Content in 28 Sawyer Core Samples.

Figure 15. SEM Photomicrographs of Uranium-Enriched Encrustations.

- A. Sample 279-522. Mineral grain with uranium-enriched encrustations absorbed onto the grain surface.
- B. Sample 279-522. Enlarged view of the uranium-enriched encrustations showing the specific encrustation from which an energy dispersion spectra was obtained.

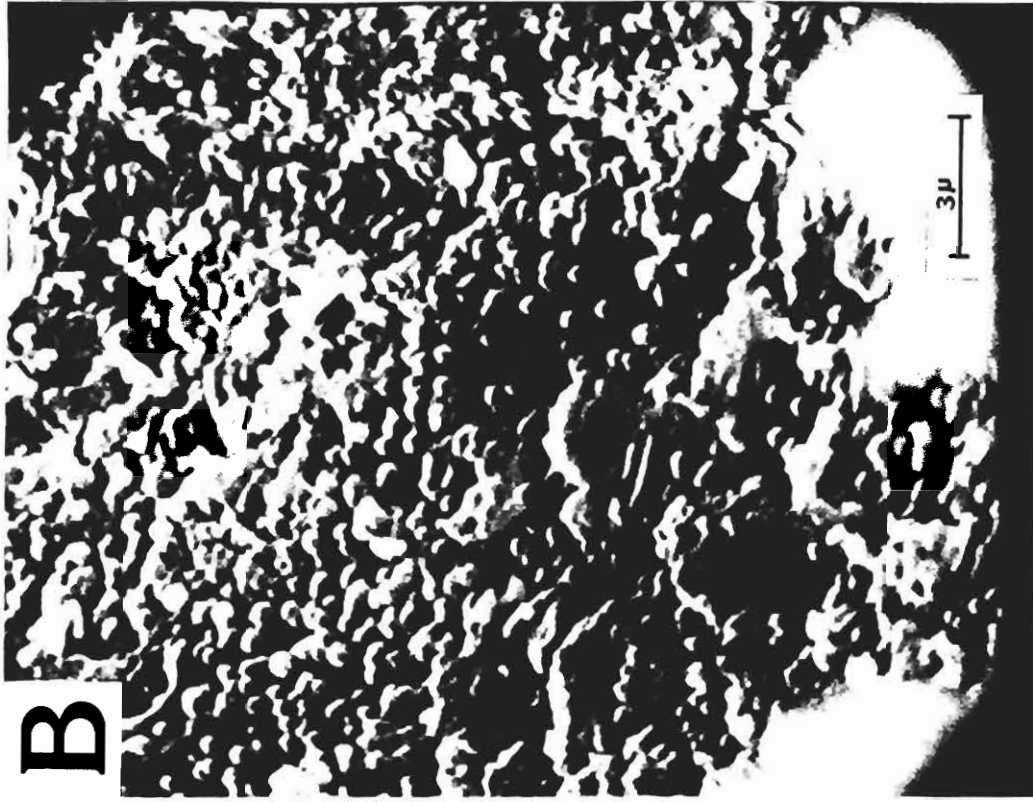
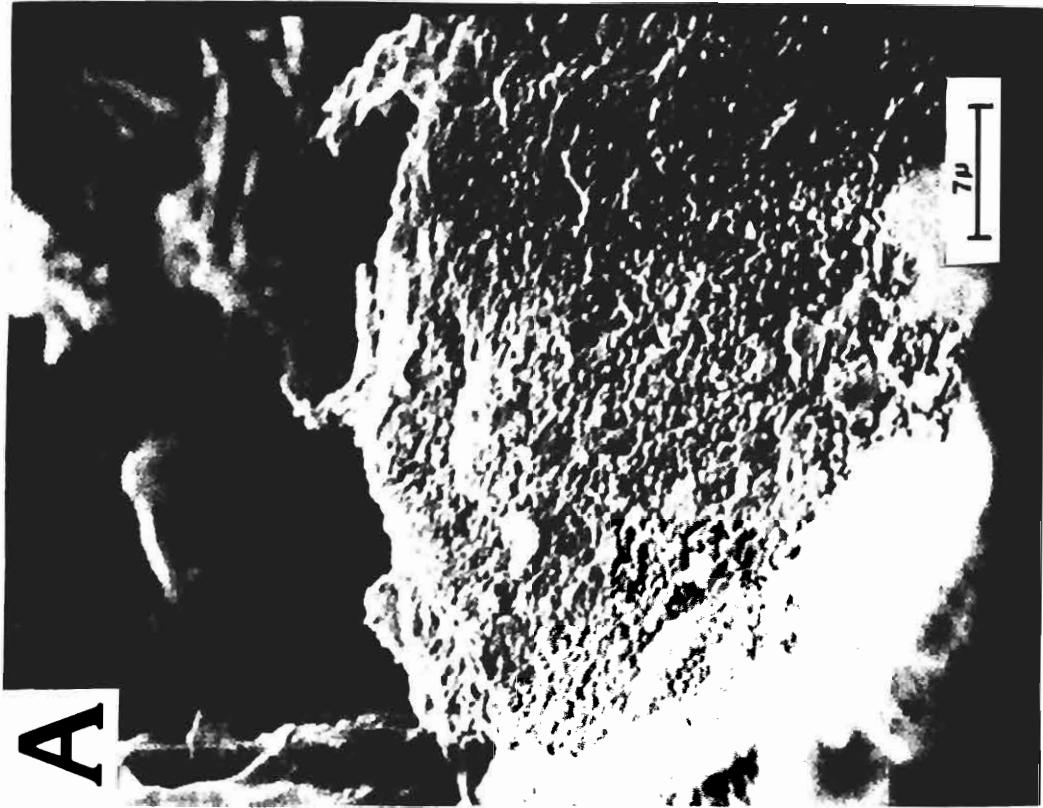


Figure 15



Figure 16. Energy Dispersion Spectra Obtained from the Encrustation Illustrated in Figure 15B. Note that the Au peaks are the result of Au coatings used for electrical conductivity across the sample.

A high grade ore sample (279-522) was examined for the presence of discrete uranium minerals using X-ray diffraction. Following the location of radioactive grains using an autoradiograph, three grains were mounted in a Gandolfi X-ray diffraction camera and were exposed to the X-ray beam for periods of 7-1/2 and 24 hours. A diffuse, scattered pattern resulted from both diffraction exposures. Therefore, uranium is inferred to occur as an adsorbed, amorphous phase and not as discrete, crystalline uranium minerals.

Opaque Mineralogy

Opaque minerals were identified by reflected-light microscopic examination of 21 polished thin sections. The opaque assemblage consists predominately of marcasite, with minor amounts of pyrite, hematite and detrital ilmenite. No uranium minerals were identified in the optical study.

V. OPAQUE TEXTURES

Framboidal Pyrite

Distinct pyrite framboids are a minor, yet significant, constituent of the opaque assemblage (Figure 17A, 18A, 18B). The framboids occur with varying degrees of marcasite replacement, ranging from total marcasite replacement to original, fresh pyrite with little or no marcasite present. Figure 17B illustrates a pair of framboids which have undergone partial replacement by marcasite, within a discontinuous pyrite shell. Pyrite framboids also appear as closely packed, botryoidal aggregates of tens of individual framboids (Figure 17C). The significance

Figure 17. Photomicrographs of Framboidal Pyrite and Sulfidized Ilmenite.
(All photomicrographs are at the same scale.)

- A. Sample 94-536. Framboidal pyrite (reflected light).
- B. Sample 94-536. Framboidal pyrite partially replaced by marcasite (reflected light, crossed nicols).
- C. Sample 214-505. Botryoidal pyrite framboids surrounded by a marcasite overgrowth (reflected light).
- D. Sample 214-508. Detrital ilmenite grain partially sulfidized to pyrite along fractures (reflected light).

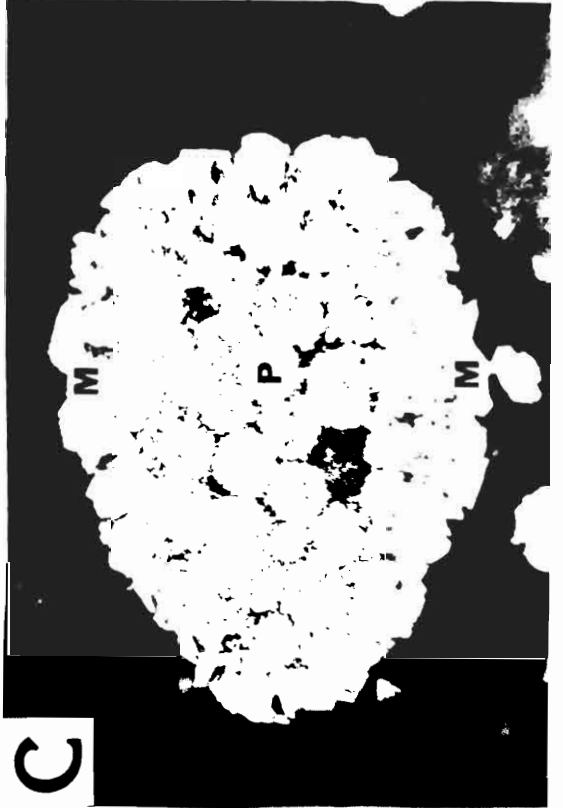


Figure 17

Figure 18. Photomicrographs of Opaque Petrology. (Photomicrographs A, C, E and B, D, F are at the same scale.)

- A. Sample 94-536. Pyrite framboids (shown by arrows) and granular marcasite in a tuff-ball conglomerate matrix (reflected light).
- B. Sample 94-536. Pyrite framboids and granular marcasite in a tuff-ball conglomerate matrix (reflected light).
- C. Sample 279-523. Selective marcasite replacement of a mineral grain (reflected light).
- D. Sample 279-523. Diffuse, irregular marcasite replacement of a mineral grain (reflected light).
- E. Sample 94-535. Coarse, multigranular marcasite (reflected light).
- F. Sample 97-490. Marcasite mineralization localized around a favorable substrate (reflected light).

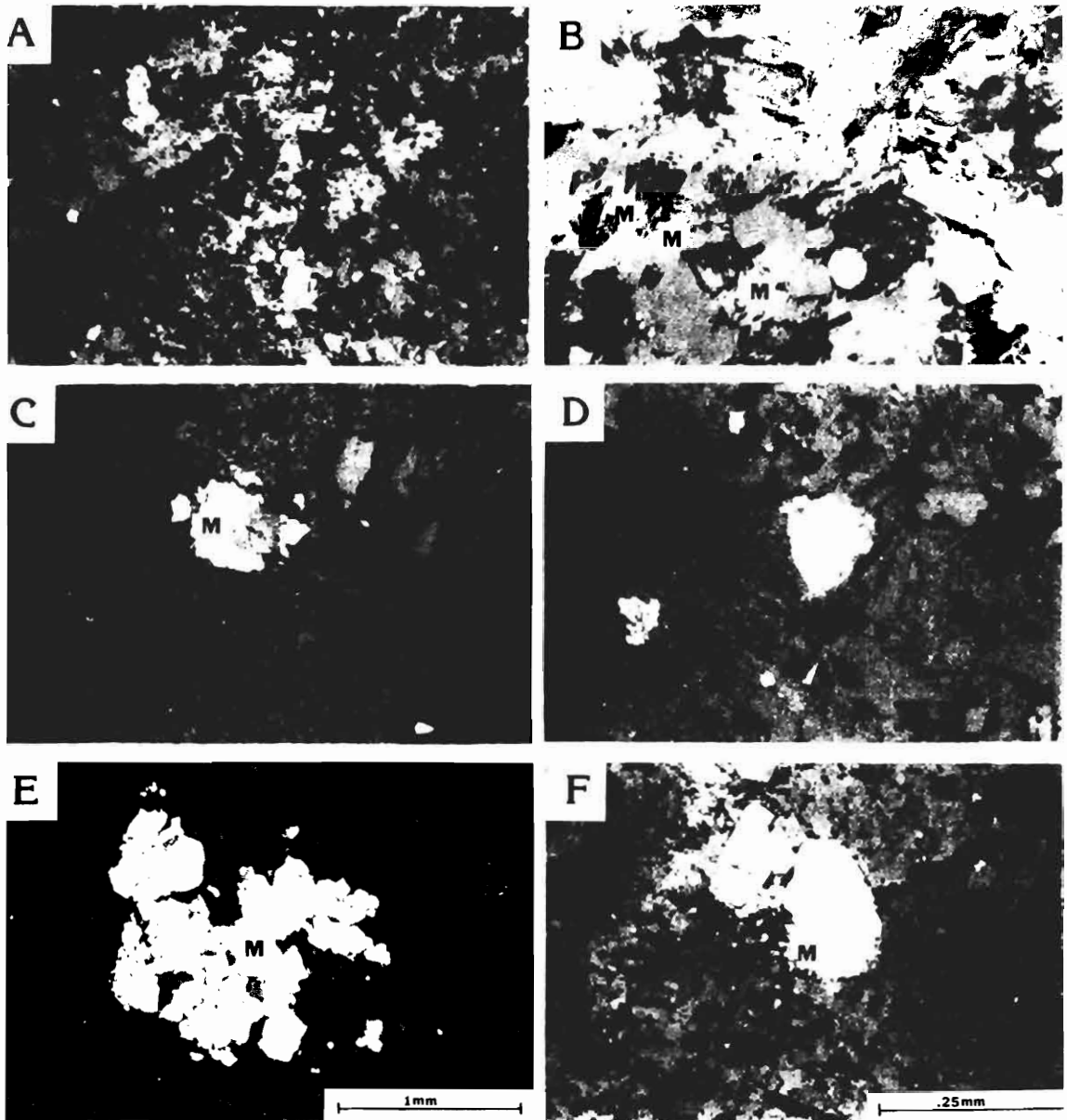


Figure 18

of framboidal pyrite to the Sawyer mineralization paragenesis will be discussed in the following chapter.

Euhedral Pyrite

Euhedral pyrite, a rare constituent of the opaque assemblage, was identified as discrete crystals in only two of the polished sections. Very finely crystalline pyrite resulting from the sulfidization of ilmenite, similar to that described by Adams et al. (1974), was also commonly observed in many of the polished thin sections (Figure 17D).

Marcasite Overgrowths and Aggregates

Marcasite occurs as overgrowths surrounding the earlier formed framboidal pyrite and as fine- to coarse-, single- to multi- grained aggregates. All of the botryoidal pyrite framboids were observed with marcasite overgrowths. This consistent relationship is evidence that marcasite was formed paragenetically later than pyrite. Marcasite was also observed as partial overgrowths around certain detrital grains (Figure 18C, 18F). Marcasite aggregates, varying in size from fine spherical grains to large multigranular aggregates, are the most common iron disulfide phase (Figure 18D, 18E). Many of these fine, spherical grains are thought to be marcasite pseudomorphic replacements of pyrite framboids.

Hematite Rims

Minor hematite rims were observed locally as borders surrounding individual tuff-ball clasts. These hematite rims were only present in strongly mineralized lithologies, representing a residual phase from

the formerly oxidized uranium alteration tongue. The majority of iron oxides associated with this alteration phase were probably sulfidized to pyrite during the post-mineralization sulfidization of the altered tongue.

Replacement

Textures indicative of replacement have been observed in volcanic rock fragments, calcite cement and detrital ilmenite. Volcanic rock fragments appear to be highly favored sites for marcasite replacement. Replacement is also suggested by local accumulations of marcasite within embayed calcite cement. Detrital ilmenite is present as fresh grains, as grains partially replaced by pyrite along fractures and as highly sulfidized, pyritized grains. The sulfidization of ilmenite implies certain geochemical conditions which will be discussed later.

VI. SULFUR ISOTOPE ANALYSIS

Sulfur isotope values are reported as deviations, $\delta^{34}\text{S}$ values, in parts per mil (0/00) from a standard according to the following relationships:

$$\delta^{34}\text{S} (0/00) = \left[\frac{\text{S}^{34}/\text{S}^{32} \text{ sample}}{\text{S}^{34}/\text{S}^{32} \text{ standard}} - 1 \right] \times 1000$$

The results of sulfur isotope analyses show values ranging from -9.9 to +8.4 $\delta^{34}\text{S}$ 0/00 and are presented in Figure 19. Analytical uncertainty of the reported values is ± 0.1 0/00 (Ripley, 1982; personal communication).

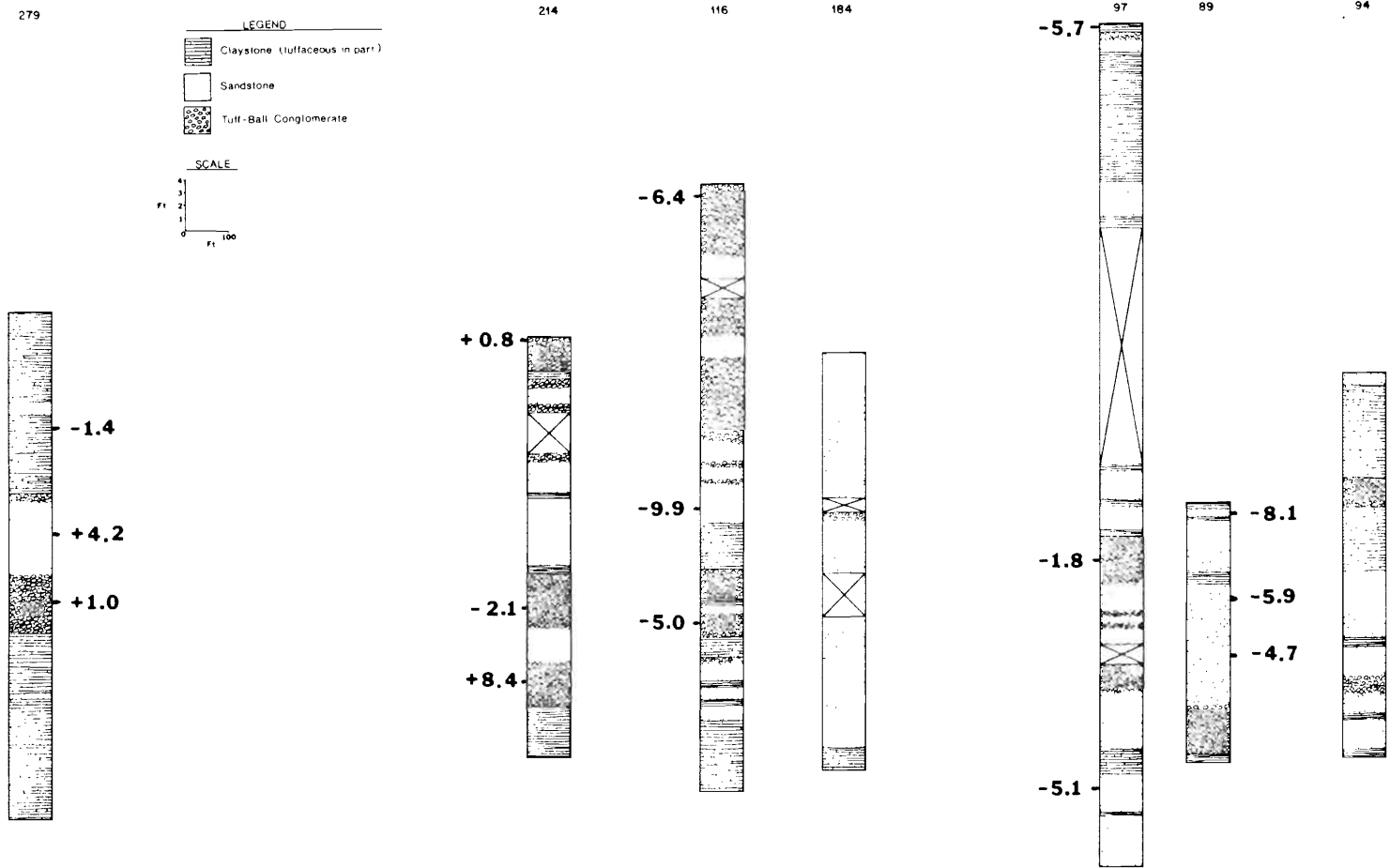


Figure 19. $\delta^{34}\text{S}$ Values for Intervals Used in the Sulfur Isotope Study of the Sawyer Cores.

CHAPTER VI

DISCUSSION

I. SOURCE OF URANIUM

Uranium Release from Volcanic Ash

The close association between rhyolitic air-fall ash and uranium deposits in south Texas has led many (Eargle and Snider, 1957; Eargle and Weeks, 1961; Eargle and Weeks, 1968; and others) to believe that ash contained within the Catahoula Formation is the principal source of uranium. Recent studies (Zelinski, 1977, 1978, 1979; Walton et al., 1981) have discussed the mechanisms involved in the leaching of uranium from ash of a rhyolitic composition. The release of uranium from the ash may proceed by one or more of the following mechanisms (Walton et al., 1981):

1. Washing and removal of an adsorbed coating of uranium, along with other metals and ions, from the surfaces of ash shards.
2. Gradual, preferential leaching of uranium during incongruent dissolution or hydrolysis.
3. Congruent solution of the glass with proportional release of uranium.
4. Release from alteration products of the glass.

This release from volcanic glass may result in either the local redistribution of uranium or long distance uranium migration, depending on the environment of dissolution.

Release Mechanisms

Comparative studies by Walton et al. (1981) between the Oligocene Tascotal and Catahoula formations contrast conditions which favor long distance migration of uranium. The Tascotal Formation has undergone open system hydrological diagenesis resulting in complete dissolution of glass shards, but uranium has only been released for local redistribution. In contrast, the Catahoula Formation has undergone both open system hydrological and vadose pedogenical diagenesis, resulting in the release of uranium for long distance transport. The study concludes that uranium is released for long distance migration only during complete solution of the glass in the vadose pedogenic environment, which occurs very early in the history of the sediments.

Uranium Release in the Sawyer Area

The release of uranium in the Sawyer area is thought to be the product of both the direct washing of adsorbed metals from ash and the dissolution of glass through pedogenic processes. The washing of adsorbed metals and ions from fresh volcanic ash of some Central American volcanoes has been documented by Taylor and Stoiber (1973). Their study shows that large amounts of ions (Mg, Zn, Cu, Mn, Cl, F, SO₄, Na, K and Ca) are released simply by rainwater percolation through the fresh ash. The release of uranium from pedogenic glass dissolution can be inferred from the depletion of uranium in paleosol horizons.

Uranium Depletion in Sawyer Paleosoils

A comparison of the uranium content in various Live Oak County petrofacies has been conducted by Galloway (1977, Table 2, page 28). Of particular interest is the depletion of uranium from the paleosoil horizons, relative to the uranium content contained in other lithologies. Galloway's analyses of nine subsurface crevasse-splay samples show an average of 4.8 ppm U_3O_8 , whereas analyses of six subsurface paleosoil horizons yielded an average of 1.5 ppm U_3O_8 . The uranium concentration within a positively identified Sawyer paleosoil horizon (core 279, 524') was found to be 2.0 ppm U_3O_8 . Thus, paleosoil horizons within, and immediately above, the Sawyer host sediments are considered to be the functional sites of glass dissolution, which, in turn, led to the release of economically significant quantities of uranium for long distance migration.

Uranium Migration

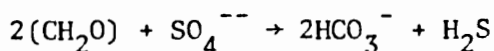
The composition of pedogenic and very early diagenetic ground waters may be inferred from the geochemical conditions that commonly occur during the subaerial diagenesis of a rhyolitic ash under semiarid climatic conditions, similar to those inferred for the Oligocene Catahoula environment (Galloway and Kaiser, 1980). The dissolution of tephra contained within paleosoil horizons in this environment probably produced oxidized, bicarbonate-rich, mildly alkaline ground waters. In addition, rainwater infiltration of periodic additions of fresh air-fall ash probably provided pulses of Na^+ , Ca^{++} , Cl^- and SO_4^{--} . These

species are presumed to have been released from the direct washing of adsorbed ions from the surfaces of newly deposited ash. Given all of the above conditions, uranium may readily form uranyl-dicarbonate complexes, with possible additional hydroxide and phosphate complexing, depending upon the pH (Langmuir, 1978). In these complexes, uranium is water soluble under oxidized conditions and would freely circulate within the local ground water flux.

II. URANIUM-SULFIDE PARAGENESIS

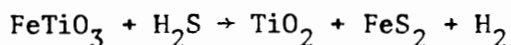
Pre-Ore Reduction of the Host Rocks

Framboidal pyrite. The pyrite framboids were present prior to the formation of the ore-stage marcasite, as marcasite overgrowths are commonly observed surrounding the framboids. Further, the presence of framboidal pyrite provides clear evidence for the pre-ore reduction of the host rocks. The distinctive framboidal morphology may arise through either organic or inorganic processes (Rickard, 1970). The organic process creates a framboid through the iron disulfide replacement of an organic vacuole or through the creation of a micro-reducing environment by sulfate-reducing bacteria. The presence of organic carbon is required in this process as a substrate for the sulfate-reducing bacteria (Goldhaber and Kaplan, 1974). Reduction of sulfate may be achieved through carbohydrate metabolism by the sulfate-reducing bacteria genus Desulfovibrio according to the following equation (Goldhaber and Reynolds, 1977):



The inorganic formation of a framboid may be achieved by the iron disulfide replacement of a pre-existing hydrogen sulfide gas bubble. Studies by Berner (1970) show that the initial replacement in either process is by an iron monosulfide, which later reacts with elemental sulfur to become an iron disulfide. The pyrite framboids observed in this study are considered to be biogenic in origin. This hypothesis may be supported by the previously described botryoidal aggregates of framboids (Figure 17C, page 41), which possibly represent pyritization of relict, degraded organic structures. The presence of residual organic carbon and sulfur isotope values also support the biogenic hypothesis.

Sulfidization of ilmenite. Detrital ilmenite grains display variable alteration to pyrite similar to the alteration described in other epigenetic uranium deposits (Adams et al., 1974; Reynolds and Goldhaber, 1978). Ilmenite is unstable in a reducing environment in which anatase is exsolved from ilmenite and the released iron then reacts with sulfur to form pyrite, according to the following equation (Adams et al., 1974):



Phase relations in the Fe-Ti-S-O-H system at 25°C shows that anatase and pyrite coexist at an Eh between 0 and -10 volts and at a pH ranging from 3 to 10 (Adams et al., 1974). Since pyrite framboids form only

at a neutral to slightly alkaline pH (Rickard, 1970), the coexistence of anatase and pyrite framboids leads to the inference that the initial reducing environment had a pH between 7 and 9 with an Eh of -2 to -6 volts. The pre-ore reduction and pyritization of the host sediments is a very important step in the preparation of a suitable uranium host rock.

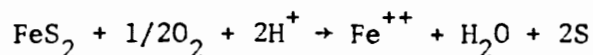
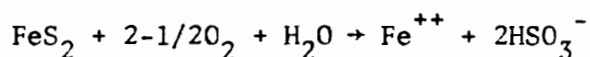
Ore-Stage Mineralization

Roll-front development. An oxidation-reduction interface was generated as oxygenated, uranium-enriched ground waters invaded the reduced, pyritic Sawyer host rocks. Uranium, and its associated dissolved trace elements that are sensitive to declining Eh-pH conditions, were precipitated along this redox boundary as a roll-front. The geochemistry of roll-front development has been investigated by many workers (Granger and Warren, 1969; Harshman, 1974; Goldhaber and Reynolds, 1977, 1978, 1979; Galloway and Kaiser, 1980; and others) and warrants further discussion with special reference to the Sawyer deposit.

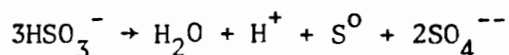
Destruction of pyrite. The importance of pyrite oxidation in creating an acidic environment associated with uranium roll-fronts has been described by Granger and Warren (1969). Their research indicates that the oxidation of pyrite, by the bacteria Thiobacillus, leads to acidic conditions at the nose of the roll-front through the generation of H^+ ions. It is important to note that substantial pyrite oxidation is required to create an acidic environment at the redox interface from a system originally consisting of alkaline ground water within alkaline host rocks. The overwhelming predominance of marcasite over

pyrite as the iron disulfide phase in the Sawyer deposit indicates that acidic conditions accompanied ore deposition. Further, the synthetic precipitation of marcasite by Rickard (1969) shows that marcasite forms only at a pH of 5.5 or less; thus, the pH of ore formation at Sawyer is inferred to have been less than 5.5.

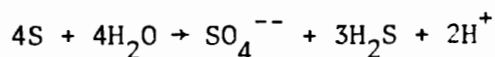
Role of unstable sulfur compounds. The oxidation of pyrite also leads to the creation of stable and unstable sulfur compounds (Granger and Warren, 1969) that greatly enhance the reducing conditions at, and immediately downdip from, the redox interface. In an acidic environment, decomposition products of pyrite oxidation include bisulfite ions (HSO_3^-) and native sulfur, according to the following equations (Granger and Warren, 1969):



Bisulfite ions are unstable and spontaneously disassociate to water, sulfur, and sulfate as follows (Granger and Warren, 1969):

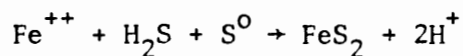


This serves to enhance both the acidity (H^+) and the reducing capacity by the generation of sulfur which hydrolizes to H_2S according to the following equation:



The production of ferrous iron, elemental sulfur and an acidic environment through the oxidation of pyrite allows for the reconstitution of iron disulfides as marcasite.

Formation of marcasite. Study of the sulfide petrology reveals that marcasite has formed through direct chemical precipitation and through the in situ replacement of framboidal pyrite. As mentioned above, the destruction of pre-ore pyrite released ferrous iron and sulfur compounds, and, upon transport into the acidic, reducing environment at the nose of the roll-front, these species combined to form ore-stage marcasite. The formation of marcasite may have proceeded according to the following equation (Berner, 1970);



This is a stepwise reaction in which FeS is formed through reaction with H_2S , followed by the reaction of FeS with S^0 to form marcasite (or pyrite, depending on the pH). The in situ conversion of pyrite framboids to marcasite requires an acidic pH and partial oxidation of pyrite. Partial oxidation of pyrite to remove a fraction of the sulfur may have produced mackinawite ($Fe_{1+x}S$). Mackinawite may then react with elemental sulfur to form marcasite (Rickard, 1969). If this was the pathway along which marcasite formed, then the conversion of mackinawite to marcasite must have been complete as no mackinawite was observed in the sulfide assemblage.

Post-Ore Re-Reduction

Sulfidization of the altered tongue. The Sawyer mineralization is enveloped in pyritized, reduced rocks both on the updip and downdip sides of the roll-front. The formerly oxidized tongue is uniformly gray and pyritic, with rare, minor residual hematite and limonite stains present locally. Regional exploration drilling conducted by Sunoco indicates that all of the formerly oxidized tongues in the Sawyer vicinity have been similarly resulfidized. This resulfidization is somewhat problematical.

Possible mechanisms for re-reduction. The phenomenon of re-reduction is not unique to the Sawyer area and has been described in association with other south Texas uranium deposits (Reynolds and Goldhaber, 1978; Galloway, 1977; and Galloway and Kaiser, 1980). There are three possible mechanisms for re-reduction:

1. The influx of H_2S gas or reducing fluids derived from hydrocarbon accumulations associated with the Oakville Fault Zone, which lies approximately six miles downdip from the Sawyer deposit.
2. The influx of H_2S from the anerobic action of sulfate-reducing bacteria in the immediately underlying and overlying sediments.
3. The influx of H_2S from petroleum-related maturation of organic material in the underlying Jackson Formation.

The analysis of sulfur isotope data from the Sawyer deposit provides some limitations on the source of sulfur for both the pre-ore and ore-stage sulfides.

Sulfur Isotope Interpretation

Previous studies. Sulfur isotope studies of several south Texas uranium deposits have been used in the interpretation of the sulfur origin and sulfide paragenesis. These studies have led to the hypothesis that many of the Catahoula-hosted uranium deposits have been precipitated directly in the presence of fault-derived H_2S . The fault-derived H_2S model was proposed by Goldhaber et al. (1978) from a sulfide petrology and sulfur isotope study of the Catahoula-hosted Benavides deposit. Uranium mineralization at Benavides occurs proximal to a prominent growth fault in sediments nearly devoid of organic carbon. In the Benavides deposit, the sulfide petrology clearly indicates pre-ore and ore stage iron disulfides in the form of pyrite and marcasite. Sulfur isotope analyses of pre-ore pyrite show that it is enriched with heavy sulfur, whereas, ore stage marcasite is enriched in isotopically light sulfur. The study concludes that pre-ore, isotopically heavy pyrite formed through the interaction of fault-derived H_2S with Fe^{2+} found within the host sandstones, whereas, ore stage, isotopically light marcasite resulted from the inorganic, chemical fractionation of heavy sulfur during the ore-forming process. This fault-derived H_2S reductant model has been subsequently invoked to explain the origin of several other south Texas deposits including: the Lamprecht (Goldhaber and Reynolds, 1979), the Felder (Goldhaber and Reynolds, 1979; Cathey, 1980), and the House-Seale deposit (Galloway and Kaiser, 1980).

However, recent sulfur isotope investigations of pre-ore, ore, and post-ore stage iron disulfides by Busche et al. (1982, unpublished manuscript) indicate that the fault-leaked H_2S model cannot be used to explain the origin of all organic deficient, south Texas deposits. Sulfur isotope studies of iron disulfides in the Benavides and Lamprecht deposits show a discrepancy in isotopic composition between the pre-ore and ore-stage sulfides. The ore-stage sulfides consistently show light sulfur isotopic compositions, whereas, pre- and post-ore iron disulfides are isotopically heavy. The heavy isotope values are similar to the isotopic compositions found in fault associated hydrocarbon accumulations indicating that the pre- and post-ore iron disulfides are consistent with the fault-derived hydrocarbon model; however, the light isotope values of the ore-stage sulfides are not. As a result, Busche et al. concluded that the sulfur isotope data do not support the hypothesis that uranium mineralization occurred directly in the presence of H_2S gas derived from fault-associated hydrocarbon reservoirs.

Sawyer prospect. The Sawyer sulfur isotope data is consistent with the sulfur isotope values compiled from several other biogenic associated uranium roll-front deposits and, therefore, may be interpreted to support a biogenic origin for the Sawyer mineralization. The range of sulfur isotope values from several previous studies is compared in Table 4 with the Sawyer data. In comparing the data, it is apparent that the Sawyer data lies within the fields of organically derived H_2S and biogenically associated uranium deposits. The Sawyer values

Table 4. Sulfur Isotope Signatures of Various Geochemical Environments.

Sulfide Source	$\delta^{34}\text{S}$	Source
1. Sawyer deposit (bulk sulfides)	+8.4 to -9.9	This study
2. Oakville fault associated gas field (Edwards)	+12.7 to +15.3	Busche et al. (1982)
3. Oakville fault associated gas field (Smackover)	+15.4 to +21.8	Busche et al. (1982)
4. Petroleum organically derived sulfide	+20 to -10	Busche et al. (1982)
5. Seawater sulfate through time	+10 to +25	Busche et al. (1982)
6. Volcanic sulfide	0 to ± 3	Busche et al. (1982)
7. 57 iron disulfide samples from Wyoming and Colorado Plateau uranium deposits (biogenic origin)	+20 to -50	Jensen (1958)
8. H_2S of organic origin	+9 to -20	Jensen (1958)
9. Benavides iron disulfides (non-ore)	+7 to +30	Goldhaber et al. (1978)
10. Benavides iron disulfides (ore)	+10 to -30	Goldhaber et al. (1978)
11. Benavides pre-ore (pyrite)	average +16	Busche et al. (1982)
12. Benavides ore- stage (marcasite)	average -28	Busche et al. (1982)

clearly do not show the heavy sulfur component associated with sulfur derived from the Oakville fault gas fields. The relatively narrow range of $\delta^{34}\text{S}$ (+8.4 to -9.9) displayed in the Sawyer values may result from a bias due to the distribution of samples along the strike of the ore body and/or from a buffering effect between pre-ore and ore stage iron disulfides.

The nature and origin of the postmineralization re-reduction is unclear. Data necessary to interpret the origin of the post-ore reductant does not exist because cores from the altered tongue of the roll-front were unavailable for study. It is logical to assume that alkaline conditions returned to the host rocks following mineralization and that under these conditions, pyrite was precipitated. The sulfur isotope composition of post-ore pyrite is perhaps the key to unraveling the source of re-reducing H_2S . It is unlikely that H_2S from the Oakville fault zone provided this post-ore reductant, in that H_2S has a strong tendency to dissociate in oxygenated, near surface, ground water, thus, it is improbable that it could have migrated six miles updip to the site of the Sawyer mineralization. It appears reasonable to assume that the re-reducing H_2S was derived from post-mineralization bacterial activity in the surrounding sediments. The validity of this hypothesis, however, remains to be tested.

Paragenesis

The uranium and iron disulfide sequence may be summarized as follows:

1. Initial reduction of the host sediments through the action of sulfate-reducing bacteria in an alkaline environment;

2. Invasion of oxygenated, alkaline, uranium-enriched ground waters into the reduced host rocks resulting in the establishment of an oxidation-reduction interface;
3. Deposition of uranium and associated trace elements along the redox interface as a roll-front accompanied by the oxidation of pyrite, concurrent decrease in pH (less than 5.5) and the reconstitution of iron disulfides as marcasite;
4. Termination of roll-front mineralization, followed by the re-reduction of the host rocks by a reductant of uncertain origin.

This paragenetic sequence is graphically displayed in Figure 20.

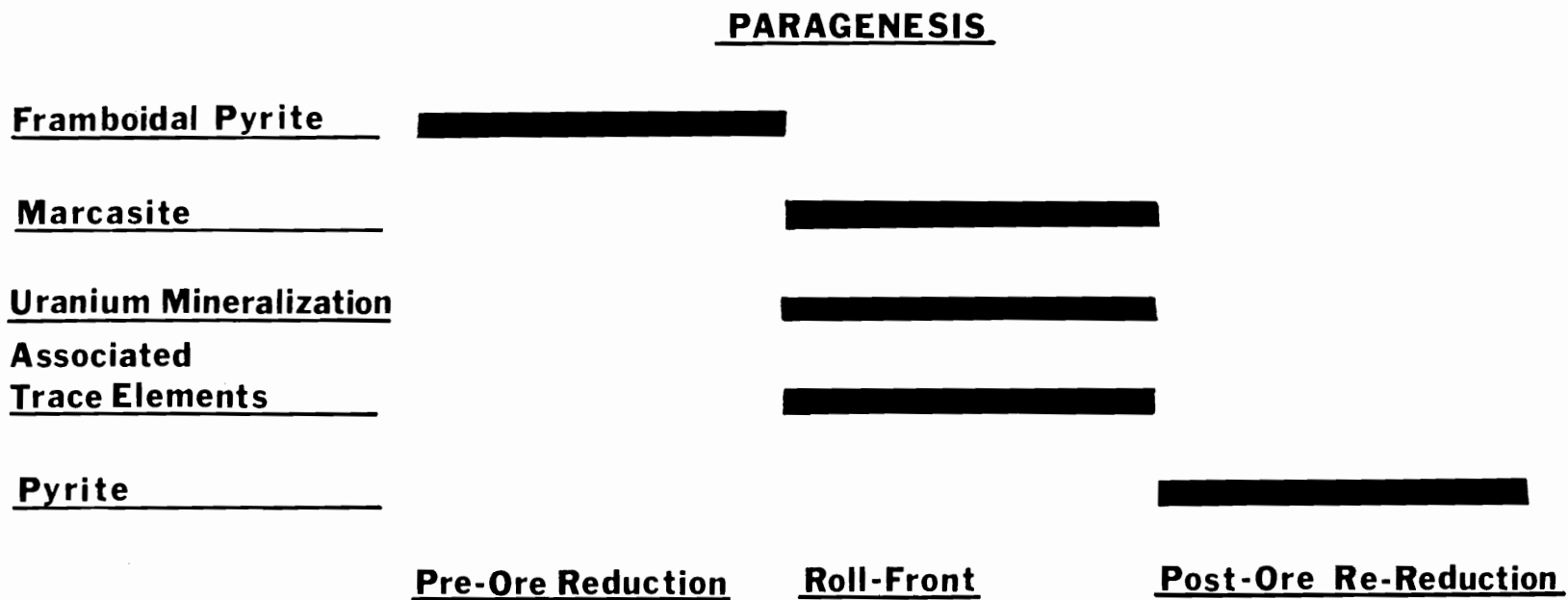


Figure 20. The Paragenesis of Sawyer Mineralization as Interpreted from Relationships Observed in the Sawyer Core Samples.

CHAPTER VII

CONCLUSIONS

The following conclusions regarding the Sawyer deposit concur with those of previously published literature:

1. The host rocks were deposited as crevasse-splay sediments derived from a major, strike-oriented, Catahoula fluvial system in northeastern Live Oak County.
2. Early pedogenic diagenetic features include clay cutans, micrite nodules and a slight argillation of the glass shards.
3. The oxidation of pre-ore pyrite produced metastable sulfur oxyanions that served to enhance the reducing environment at the nose of the roll-front and created an acidic pH.
4. Post-mineralization diagenesis resulted in the precipitation of zeolites and sparry, pore-filling calcite cement.
5. Minor, late-stage calcite cement cemented most of the residual pore space, effectively sealing the remaining porosity such that the system has remained static since diagenesis.

In addition, the following conclusions regarding the Sawyer prospect have resulted from this study:

1. Shallow burial of the sedimentary sequence resulted in the initial sulfidization of the sediments by the activities of sulfate-reducing bacteria.

2. Invasion of oxygenated, alkaline, uranium-enriched ground waters into the reduced sediments produced a redox interface along which uranium and associated trace minerals were precipitated.
3. Ore-stage iron disulfides were precipitated as fine- to coarse-grained marcasite and included marcasite replacement and overgrowths surrounding pre-ore framboidal pyrite.
4. The sulfur isotope data is consistent with a biogenic origin of the deposit.
5. The Sawyer data does not support the hypothesis that the Oakville Fault Zone provided the ore-stage reductant as suggested by Galloway and Kaiser (1980).
6. Post-ore re-reduction of the altered tongue was accomplished by a reductant of uncertain origin.

LIST OF REFERENCES

LIST OF REFERENCES

- Adams, S. S., Curtis, H. S., and Hafen, P. L., 1974, Alteration of detrital magnetite-ilmenite in continental sandstones of the Morrison formation, New Mexico, in Formation of Uranium Ore Deposits, IAEA, Vienna, pp. 219-253.
- Berner, R. A., 1970, Sedimentary pyrite formation: *Am. Jour. Sci.*, v. 268, no. 4, pp. 1-23.
- Busche, F. D., Goldhaber, M. B., and Reynolds, R. L., 1982, Fault leaked H₂S and the origin of south Texas uranium deposits: Implications of sulfur isotope studies: Unpublished Manuscript, presented at the south Texas AIME meeting, Dallas, February, 1982.
- Cathey, W. B., 1980, Implications of the geology and geochemistry of the Maclean Five uranium deposit, Three Rivers, Texas: Unpublished Master's Thesis, The University of Tennessee, Knoxville, 126 pp.
- Coleman, J. M., 1969, Brahmaputra River: Channel processes and sedimentation: *Sed. Geology*, v. 3, pp. 129-239.
- Dailly, G. C., 1976, A possible mechanism relating progradation, growth faulting, clay diapirism and overthrusting in a regressive sequence of sediments: *Bull. of Canadian Petroleum Geology*, v. 24, no. 1, pp. 92-116.
- Eargle, D. H., and Snider, J. L., 1956, A preliminary report on the stratigraphy of the uranium bearing rocks of the Karnes County area, south-central Texas: U. S. Geol. Survey Report TEI-488, 46 pp.
- Eargle, D. H., and Weeks, A. D., 1961, Possible relation between hydrogen sulfide-bearing hydrocarbons in fault-line oil fields and uranium deposits in the southeast Texas coastal plain: U. S. Geol. Survey Prof. Paper 424-D, pp. 7-9.
- Eargle, D. H., and Weeks, A. D., 1968, Factors in the formation of uranium deposits, coastal plain of Texas: *South Texas Geol. Soc. Bull.* 9, no. 3, pp. 3-13.
- Fisher, W. L., 1973, Deltaic sedimentation, salt mobilization and growth faulting in the Gulf Coast basin: *Am. Assoc. of Petroleum Geologists Bull.*, v. 57, no. 4, p. 779.
- Folk, R. L., 1974, *Petrology of sedimentary rocks*: Austin, Hemphill Publishing Company, 182 pp.

- Galloway, W. E., 1977, Catahoula formation of the Texas coastal plain: Depositional systems, composition, structural development, groundwater flow history and uranium distribution: The University of Texas at Austin, Bureau of Economic Geology Report of Investigations, no. 87, 59 pp.
- Galloway, W. E., and Kaiser, W. R., 1980, Catahoula formation of the Texas coastal plain: Origin, geochemical evolution and characteristics of uranium deposits: The University of Texas at Austin, Bureau of Economic Geology Report of Investigations, no. 100, 81 pp.
- Goldhaber, M. B., and Kaplan, I. R., 1974, The sulfur cycle, in The Sea, vol. 5, Goldberg, E., ed., Marine Chemistry: New York, John Wiley and Sons, Inc., pp. 569-655.
- Goldhaber, M. B., and Reynolds, R. L., 1977, Geochemical and mineralogical studies of a south Texas roll-front uranium deposit: U. S. Geology Surv. Open-File Report 77-821, 34 pp.
- Goldhaber, M. B., Reynolds, R. L., and Rye, R. O., 1978, Origin of a south Texas roll-type uranium deposit: II. Petrology and sulfur isotope studies: Economic Geology, v. 73, pp. 1690-1705.
- Granger, H. C., and Warren, C. G., 1969, Unstable sulfur compounds and the origin of roll-type uranium deposits: Economic Geology, v. 64, pp. 169-171.
- Jensen, M. L., 1958, Sulfur isotopes and the origin of sandstone-type uranium deposits: Economic Geology, v. 53, pp. 598-616.
- Jones, P. H., and Wallace, R. H., Jr., 1974, Hydrogeologic aspects of structural deformation in the northern Gulf of Mexico basin: U. S. Geol. Surv. Jour. Research, v. 2, no. 5, pp. 511-517.
- Klohn, M. L., and Pickens, W. R., 1970, Geology of the Felder deposits, Live Oak County, Texas: Mining Engineers Soc. Reprint, no. 7-1-38, 19 pp.
- Langmuir, D., 1978, Uranium solution-mineral equilibrium at low temperatures with application to sedimentary ore deposits: *Geochimica et Cosmochimica Acta*, v. 42, no. 6, pp. 547-569.
- McBride, E. F., Lindemann, W. L., and Freeman, P. S., 1968, Lithology and petrology of the Gueydan (Catahoula) formation in south Texas: The University of Texas at Austin, Bureau of Economic Geology Report of Investigations, no. 63, 122 pp.
- Reynolds, R. L., and Goldhaber, M. B., 1978, Origin of a south Texas roll-type uranium deposit: I. Alteration of iron-titanium oxide minerals: Economic Geology, v. 73, pp. 1677-1689.

- Rickard, D. T., 1969, The chemistry of iron sulphide formation at low temperatures: Stockholm Contributions in Geology, v. 20, no. 4, pp. 67-95.
- Rickard, D. T., 1970, The origin of framboids: Lithos 3, pp. 269-293.
- Taylor, P. S., and Stoiber, R. E., 1973, Soluable material on ash from active Central American volcanoes: Geol. Soc. of Am. Bull., v. 84, pp. 1031-1042.
- Walton, A. W., Galloway, W. E., and Henry, C. D., 1981, Release of uranium from volcanic glass in sedimentary sequences: An analysis of two systems: Economic Geology, v. 76, pp. 69-88.
- Zielinski, R. A., 1977, Uranium mobility during interaction of rhyolitic glass with alkaline solutions: U. S. Geol. Survey Open-File Report 77-744, 36 pp.
- Zielinski, R. A., 1978, Uranium abundances and distribution in associated glassy and crystalline rhyolites of the western United States: Geol. Soc. of Am. Bull., v. 78, pp. 409-414.
- Zielinski, R. A., 1979, Uranium mobility during interaction of rhyolitic obsidian, perlite, and feldspar with alkaline carbonate solution: T=120°C, P=210 kg/cm²: Chemical Geology, v. 27, pp. 47-63.

VITA

Charles Leonard Brewster was born in Painesville, Ohio, on June 19, 1953. He graduated from Madison Memorial High School, Madison, Ohio, in June 1971. Following high school, he enrolled at Miami University, Oxford, Ohio, and received a B.A. degree in geology in August 1975. After graduation from Miami, he was employed as a uranium exploration geologist for Wold Minerals Company, Casper, Wyoming (1975-1977); Texaco, Inc., Corpus Christi, Texas (1977-1978); Sunoco Energy Development Company, Dallas, Texas (1978-1980). During the fall of 1980, he enrolled in the Economic Geology program at The University of Tennessee in Knoxville and received an M.S. degree in geology in December 1982. Following graduation, he accepted employment as an exploration geologist with Amoco Production Company, New Orleans, Louisiana. He is married to the former Renee L. Harrison of Grand Rapids, Michigan.